CANMET

Canada Centre for Mineral and Energy Technology

Centre canadien de la technologie des minéraux et de l'énergie

Mining Research Laboratories

Laboratoires de recherche minière

Energy, Mines and Resources Canada

Énergie, Mines et Ressources Canada

Canada

THE ENERGY OF OUR RESOURCES · THE POWER OF OUR IDEAS

L'ENERGIE DE NOS RESSOURCES · NOTRE FORCE CREATRICE

Laboratory Characterization of the Underground Research Laboratory's 420 m Level: Borehole 409-031-MS9

R. Jackson

MRL 92-007(TR) January 1992

54 pp

MICROMEDIA

Laboratory Characterization of the Underground Research Laboratory's 420 m Level: Borehole 409-031-MS9

by

R. Jackson[1]

Abstract

Laboratory testing of rock core obtained from borehole 409-031-MS9 was undertaken in support of the mineby experiment to be conducted on the 420 m level of AECL Research's Underground Research Laboratory. As anticipated, the strength of the rock was observed to increase with increasing confining pressure, rising from a mean unconfined strength of 170 MPa to 598 MPa at a confining pressure of 60.0 MPa. Tangent moduli determined at 40% and 50% of the peak deviator stress tended to increase with increasing confining pressure up to 30 MPa. Increasing confining pressures beyond 30 MPa, however, had little effect with the 40% and 50% tangent moduli plateauing out at approximately 69.50 GPa and 66.00 GPa, respectively. Poisson's ratios, also determined at 40% and 50% of the peak deviator stress, showed little variation over the confining pressure range exhibiting mean values of 0.33 and 0.40, respectively.

A novel method of analysis comparing the linear-elastic behaviour of the rock with that actually observed during loading indicated that the onset of new crack formation and propagation for this rock type occurs at approximately 43% of the peak deviator stress regardless of the level of confinement.

[1] Physical Scientist, Canadian Mine Technology Laboratory, Mining Research Laboratories, CANMET, Energy, Mines and Resources Canada, Ontario.

Keywords

Rock Properties, Mechanical, Young's Modulus, Poisson's Ratio, Uniaxial Compressive Strength, Hoek and Brown

Caractérisation en laboratoire du niveau 420 m du Laboratoire de recherche souterrain : Trou de sondage 409-031-MS9

par

R. Jackson[1]

Résumé

Les essais réalisés en laboratoire sur la carotte prélevée dans le trou de sondage 409-031-MS9 ont été entrepris pour appuyer les expériences que doit réaliser le Laboratoire de recherche souterrain de l'EACL. Comme prévu, lorsque la pression de confinement est accrue, la résistance de la roche augmente, passant d'une résistance non confinée moyenne de 170 MPa à 598 MPa à la pression de confinement de 60,0 MPa. Les modules tangents déterminés à 40 % et 50 % de la contrainte déviatrice maximale ont tendance à augmenter lorsqu'on accroît la pression de confinement jusqu'à 30 MPa. L'accroissement des pressions de confinement au-delà de 30 Mpa, cependant, a peu d'effet lorsque 40 % et 50 % des modules tangents atteignent un plateau à environ 69,50 GPa et 66,00 GPa, respectivement. Les coefficients de Poison, déterminés également à 40 % et 50 % de la contrainte déviatrice maximale, ont indiqué peu de variation dans l'intervalle des pressions de confinement, leurs valeurs moyennes étant respectivement de 0,33 et de 0,40.

Un nouvelle méthode d'analyse qui consiste à comparer le comportement élastique linéaire de la roche avec celui réellement observé durant le chargement révèle que les fissures se forment et se propagent dans ce type de roche lorsque la contrainte déviatrice atteint 43 % de sa valeur maximale, quel que soit le niveau de confinement.

[1] Physicien, Laboratoire canadien de la technologie minière, Laboratoires de recherche minière, CANMET, Énergie, Mines et Ressources Canada (Ontario).

Termes clés
Propriétés mécaniques des roches, module de Young, coefficient de Poisson, résistance à la compression uniaxiale, Hoek et Brown

Contents

ABSTRACT i
RESUME ii
INTRODUCTION 1
SAMPLING AND SPECIMEN PREPARATION 1
TEST APPARATUS AND PROCEDURE 3
TESTING PROGRAM 4
RESULTS AND DISCUSSION 4
Test Results 4
Failure Deviator Stress 8
Tangent Modulus of Elasticity 16
Poisson's Ratio 17
CONCLUSIONS AND RECOMMENDATIONS 17
ACKNOWLEDGEMENTS 19
REFERENCES 19
APPENDIX A 21

Tables

1. Dimensions and densities 2
2. Summary of mechanical properties 5
3. Fracture characteristics code 7
4. Summary of mean mechanical properties 9

Figures

1. Failure deviator stress versus confining pressure 11
2. Dilational stress versus confining pressure 11

3. Mohr-Coulomb and Hoek and Brown failure criteria analyses, peak deviator stress . . 13
4. Mohr-Coulomb and Hoek and Brown failure criteria analyses, dilational stress 14
5. 40% tangent modulus versus confining pressure 15
6. 50% tangent modulus versus confining pressure 15
7. 40% Poisson's ratio versus confining pressure 18
8. 50% Poisson's ratio versus confining pressure 18

Introduction

The Canadian Nuclear Fuel Waste Management Program (CNFWMP) is concerned with the safe, long term disposal of high level nuclear wastes in vaults located at depth in plutonic rock. As part of the program, Atomic Energy of Canada Limited (AECL) has constructed the Underground Research Laboratory (URL) located near Lac du Bonnet, Manitoba to provide a representative environment in which to conduct in situ investigations. Some of these investigations will provide rock mass mechanical properties and will assess the accuracy of mathematical models by comparison with field measurements (Simmons and Soonawala, 1982). In support of these investigations, a joint laboratory testing and analysis program has been undertaken by the Canada Centre for Mineral and Energy Technology (CANMET) and AECL to provide data on the mechanical properties of the rock mass surrounding the URL excavation.

Among the investigations planned for the URL is the 420 m level mine-by experiment (Simmons, 1990). An important facet of the study involves predicting the response of the rock mass in the effected area of the mine-by for comparison with actual measurements taken during excavation. This report summarizes the results of a laboratory test program conducted on samples obtained from the immmediate vicinity of the mine-by. These will subsequently be used as mechanical property input for predictive models.

Sample and Specimen Preparation

Core used in these tests was supplied by AECL and obtained from Borehole 409-031-MS9 between the downhole lengths of 8.80 and 12.85 m. The rock is a massive, grey, medium to coarse grained granite, composed of quartz, K-feldspar, plagioclase and biotite. Specimens with ends ground parallel to within 0.025 mm were prepared from the core in accordance to procedures described in the Pit Slope Manual Supplement 3-5 (Gyenge and Ladanyi, 1977) and suggested by the International Society for Rock Mechanics (Brown, 1981).

The lengths, diameters and bulk densities of the specimens are shown in Table 1. The lengths

Table 1 - Dimensions and densities of specimens

Specimen Identification No.	Diameter (mm)	Length (mm)	Density (Mg/m^3)
409-031-MS9 8.800	44.83	101.54	2.65
8.900	44.83	101.89	2.65
9.077	44.80	101.84	2.63
9.185	44.80	102.72	2.63
9.369	44.82	98.15	2.64
9.475	44.82	101.37	2.63
9.581	44.83	101.80	2.63
9.720	44.83	102.06	2.64
9.827	44.84	102.13	2.64
9.933	44.83	101.42	2.64
10.142	44.82	100.89	2.64
10.250	44.84	101.85	2.64
10.386	44.85	101.17	2.64
10.598	44.83	102.01	2.64
10.705	44.83	101.55	2.64
11.040	44.84	101.33	2.64
11.149	44.85	100.35	2.66
11.257	44.85	101.72	2.64
11.367	44.86	102.66	2.63
11.475	44.85	101.07	2.63
11.650	44.86	102.00	2.63
11.759	44.88	101.25	2.65
11.865	44.88	102.24	2.64
12.421	44.86	102.65	2.64
12.532	44.86	101.36	2.65
12.635	44.88	101.13	2.64
12.744	44.84	99.52	2.65
12.849	44.89	100.68	2.63

of the specimens varied from 98.15 to 102.72 mm with diameters in the range of 44.80 to 44.89 mm, (length to diameter ratio of approx. 2.2:1).

The four specimens used for uniaxial compression tests as well as one at each confining pressure were strain gauged using Micro-measurements type EA-06-500BH-120 gauges. Two diametrically opposed axial strain gauges were mounted at the mid-height of each of the specimens and were connected in series to form a single active gauge. Two circumferential strain gauges were similarly mounted 90° to the axial gauges.

Test Apparatus and Procedure

An MTS 815 Rock Mechanics Test System was used to carry out the uniaxial and triaxial compression tests. The system includes a servo-hydraulic press consisting of a 2.22 MN rated load cell, load frame, hydraulic power supply, triaxial cell, test controller, test processor, and DEC micro PDP 11/73 computer. The triaxial cell is equipped with three linear variable differential transducers (LVDTs) for the measurement of axial strain and an extensometer with a circumferential kit for the measurement of circumferential strain. For a detailed description of the MTS system and its operation, the reader is referred to the MTS Operation Manual (MTS Systems Corp., 1986) and CANMET Division Report MRL 87-33(INT) (Gorski, 1987).

The procedure used to conduct the uniaxial compression tests conformed with methods recommended in the Pit Slope Manual Supplement 3-2 (Gyenge and Herget, 1977). The axial and circumferential strain gauges mounted on the specimen were connected to B&K type 1526 strain indicators in a half-bridge configuration. The indicators' outputs were monitored every three seconds by the test processor in the MTS system. LVDTs in the triaxial cell were also used to measure axial displacement.

The instrumented (LVDTs and extensometer) rock specimen was placed in the triaxial cell which was subsequently filled with Syltherm 800 heat transfer fluid. The confining pressure and the axial load were then raised simultaneously to the prescribed test level. The specimens were then axially loaded to failure at a constant rate of 0.75 MPa per second under computer control.

Signals from the load cell, LVDTs, extensometer and strain gauges were scanned by the computer every three seconds. The signals were converted to engineering units and measurements from the LVDTs were corrected for end platen compression. The data were stored on hard disk in the micro PDP 11/73 computer and later transferred to a micro-computer for data analysis and plotting.

Testing Program

Testing took place at the Canadian Mine Technology Laboratory, Mining Research Laboratories, CANMET, Energy, Mines and Resources Canada in Ottawa in September, 1991. The testing program consisted of twenty-eight specimens, four of which were tested at each of the following confining pressures; 0.1, 10.0, 20.0, 30.0, 40.0, 50.0 and 60.0 MPa. The mechanical properties determined for each specimen are summarized in Table 2.

Results and Discussion

Test Results

Table 2 summarizes the failure deviator stress, dilational stress, as well as, the tangent Young's moduli and Poisson's ratios determined at stress levels equivalent to 40% and 50% of the peak deviator stress for each specimen. In those instances where strain gauges were used to measure the axial and circumferential strains, the tangent Young's moduli and Poisson's ratios were determined using those measurements. Otherwise, LVDT and extensometer measurements were used. The Young's modulus values were determined using stress/strain data between 30% and 60% of the peak deviator stress to perform a cubic fit of the form;

$$\sigma = a_0 + a_1\varepsilon + a_2\varepsilon^2 + a_3\varepsilon^3 \qquad (1)$$

where; σ = stress (MPa)

ε = strain

and a_0, a_1, a_2 and a_3 are coefficients

Table 2 - Summary of mechanical properties

Specimen Identification	Confining Pressure (MPa)	Peak Deviator Stress (MPa)	Dilational Stress (MPa)	40% Tangent Modulus (GPa)	40% Poisson's Ratio	50% Tangent Modulus (GPa)	50% Poisson's Ratio	Failure Angle (°)	Failure Characteristics
409-031-MS9 8.800	0.1	170	75	52.70	0.34	55.06	0.42	N/A	MAC
9.720	0.1	164	72	59.02	0.36	61.09	0.43	N/A	MAC
10.598	0.1	175	74	54.51	0.28	55.88	0.36	65	MSY
11.650	0.1	171	76	55.76	0.30	55.76	0.37	N/A	MAC
8.900	10.0	297	147	70.51	0.38	63.92	0.42	67	2CY
9.827	10.0	302	129	62.84	0.31	61.88	0.41	67	2SY
10.705	10.0	318	134	63.67	0.32	63.15	0.44	69	2SX
11.759	10.0	293	123	61.51	0.31	60.65	0.42	68	MSY
9.077	20.0	393	174	66.12	0.39	63.42	0.45	65	2SX
9.933	20.0	394	171	67.83	0.33	64.89	0.44	67	2SY
11.040	20.0	402	170	66.73	0.32	64.18	0.43	67	2SY
11.865	20.0	383	173	64.60	0.33	62.55	0.40	71	2CK
9.185	30.0	473	220	70.36	0.33	66.51	0.38	67	2SX
10.142	30.0	474	192	68.20	0.33	65.02	0.43	66	2SY
11.149	30.0	448	197	69.68	0.32	66.32	0.39	69	2SX
12.421	30.0	455	191	68.73	0.35	65.47	0.43	69	2SY
9.369	40.0	497	228	72.38	0.33	68.52	0.38	71	2CY
10.250	40.0	521	221	70.81	0.34	66.48	0.41	66	2SY
11.257	40.0	519	219	71.32	0.30	67.54	0.39	60	2SX
12.532	40.0	504	217	69.17	0.34	65.67	0.41	71	3SY

Table 2 - cont'd

Specimen Identification	Confining Pressure (MPa)	Peak Deviator Stress (MPa)	Dilational Stress (MPa)	40% Tangent Modulus (GPa)	40% Poisson's Ratio	50% Tangent Modulus (GPa)	50% Poisson's Ratio	Failure Angle (°)	Failure Characteristics
409-031-MS9 9.475	50.0	568	239	69.36	0.37	65.39	0.42	63	3SY
10.386	50.0	571	241	69.64	0.34	65.87	0.40	69	2SX
11.367	50.0	582	256	68.61	0.32	64.77	0.39	64	MSY
12.635	50.0	554	231	69.39	0.29	65.60	0.39	64	MSY
9.581	60.0	593	266	68.07	0.30	64.60	0.35	67	2SX
11.475	60.0	623	277	69.76	0.32	65.82	0.38	74	2SY
12.744	60.0	576	253	68.57	0.35	64.98	0.41	66	2SX
12.849	60.0	599	245	69.89	0.30	64.26	0.38	67	2SX

Table 3 - Fracture characteristics code

Character	Code	Description
First	numeric	number of fragments
	M	multiple
	X	no description
Second	A	axial cracks
	C	curved fracture
	F	fracture
	I	irregular fracture
	J	conjugate fractures
	K	cracks
	P	planar fracture
	S	shear fracture
	T	stepped shear fracture
	U	unconnected and stepped fracture
	V	vertical cracks
	X	no description
Third	B	wedge-shaped bottom end
	C	conical top and bottom ends
	K	cracks
	M	conical bottom end
	P	conical top end
	T	wedge-shaped top end
	W	wedge-shaped top and bottom ends
	X	no description
	Y	splays

Strains corresponding to 40% and 50% of the peak deviator stress are then substituted into the first derivative of the best fit equation to determine its instantaneous slope and, therefore, its tangent modulus. Poisson's ratios were determined from the ratio of the circumferential to the axial tangent moduli.

In addition, Table 2 contains the failure angle, ϕ (if measureable) and the failure characteristics observed for each specimen. The failure characteristics code used in Table 2 refers to that outlined in the mechanical rock property data base and is defined in Table 3.

Stress versus axial strain, circumferential strain and volumetric strain curves for all tests are presented in Appendix A. Also included in the figures is a curve which illustrates the deviation between the volumetric stress/strain actually exhibited by the samples and that which would be anticipated from purely elastic considerations. The curve was constructed using the 40% Young's modulus and Poisson's ratio determined for each specimen (presumably when the specimen is behaving in a linear elastic fashion). These values were used to determine what the elastic volumetric strain would be throughout the stress range used during testing. The actual volumetric strain is then compared to this and the incremental deviation between the two is plotted against stress.

Failure Deviator Stress

The variation of the mean failure deviator stress, $(\sigma_1-\sigma_3)$, with confining pressure, σ_3, is illustrated in Figure 1 and summarized in Table 4 and, as anticipated, it was observed to increase as σ_3 increased.

In addition to determining the peak or failure deviator stress, investigators at the URL are utilizing the deviation of linear-elastic volumetric strain curve described earlier to estimate the long-term strength of the URL granite. The deviation observed during initial loading is caused by crack closure. This is followed by a region exhibiting little or no difference from linear-elastic behaviour. Finally, the deviation begins to increase indicating crack formation and propagation. The long-term strength, then, is considered to be that point where the actual

Table 4 - Summary of mean mechanical properties

Specimen Identification	Confining Pressure (MPa)	Peak Deviator Stress (MPa)	Dilational Stress (MPa)	40% Tangent Modulus (GPa)	40% Poisson's Ratio	50% Tangent Modulus (GPa)	50% Poisson's Ratio
409-031-MS9 8.800m - 12.849m	0.1	170 (5)	74 (2)	55.50 (2.66)	0.32 (0.04)	56.95 (2.79)	0.40 (0.04)
	10.0	302 (11)	133 (10)	64.63 (4.02)	0.33 (0.03)	62.40 (1.44)	0.42 (0.01)
	20.0	393 (8)	172 (2)	66.32 (1.35)	0.34 (0.03)	63.76 (1.01)	0.43 (0.02)
	30.0	462 (13)	200 (14)	69.24 (0.96)	0.33 (0.01)	65.83 (0.70)	0.41 (0.03)
	40.0	510 (12)	221 (5)	70.92 (1.34)	0.33 (0.02)	67.05 (1.24)	0.40 (0.02)
	50.0	569 (12)	242 (10)	69.25 (0.44)	0.33 (0.03)	65.41 (0.47)	0.40 (0.01)
	60.0	598 (19)	260 (14)	69.07 (0.89)	0.32 (0.02)	64.92 (0.67)	0.38 (0.02)

specimen behaviour begins to deviate from linear-elastic behaviour and new crack growth is initiated. Figure 2 and Table 4 summarize the mean long-term strength or `dilational strength´ determined at each confining pressure. Again, as might be expected, the dilational strength increased with increasing confining pressure. It is interesting to note that the apparent dilational strength is consistently close to 43% of the peak deviator stress for this rock type with a standard deviation of 2% over the sample population used for this test program.

The strength properties of intact rock material can be expressed in terms of the Hoek and Brown failure criterion. The empirical relationship developed by Hoek and Brown (1980) between the principal stresses associated with the failure of a rock is given as follows:

$$\sigma_1 = \sigma_3 + \sqrt{m\sigma_c\sigma_3 + s\sigma_c^2} \qquad (2)$$

where σ_1 = major principal stress at failure

σ_3 = minor principal stress

σ_c = predicted uniaxial compressive strength

m and s are constants of the rock substance

The values of m and s depend on the properties of the rock and the extent to which the rock has been broken before being subjected to the principal stresses σ_1 and σ_3. For an intact rock, s = 1, and a predicted uniaxial compressive strength, σ_c, and the material constant m can be computed using the following equations:

$$\sigma_c^2 = \frac{\Sigma y_i}{n} - \left[\frac{\Sigma x_i y_i - \frac{\Sigma x_i \Sigma y_i}{n}}{\Sigma x_i^2 - \frac{(\Sigma x_i)^2}{n}} \right] \frac{\Sigma x_i}{n} \qquad (3)$$

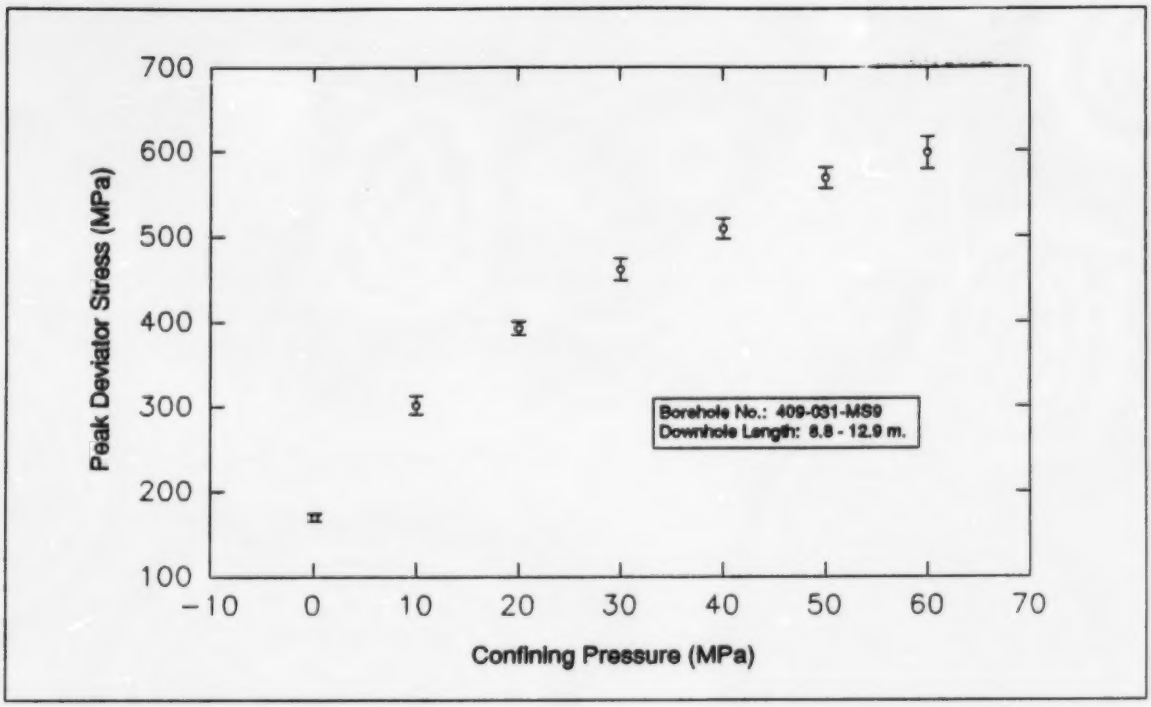

Figure 1 - Failure Deviator Stress versus Confining Pressure

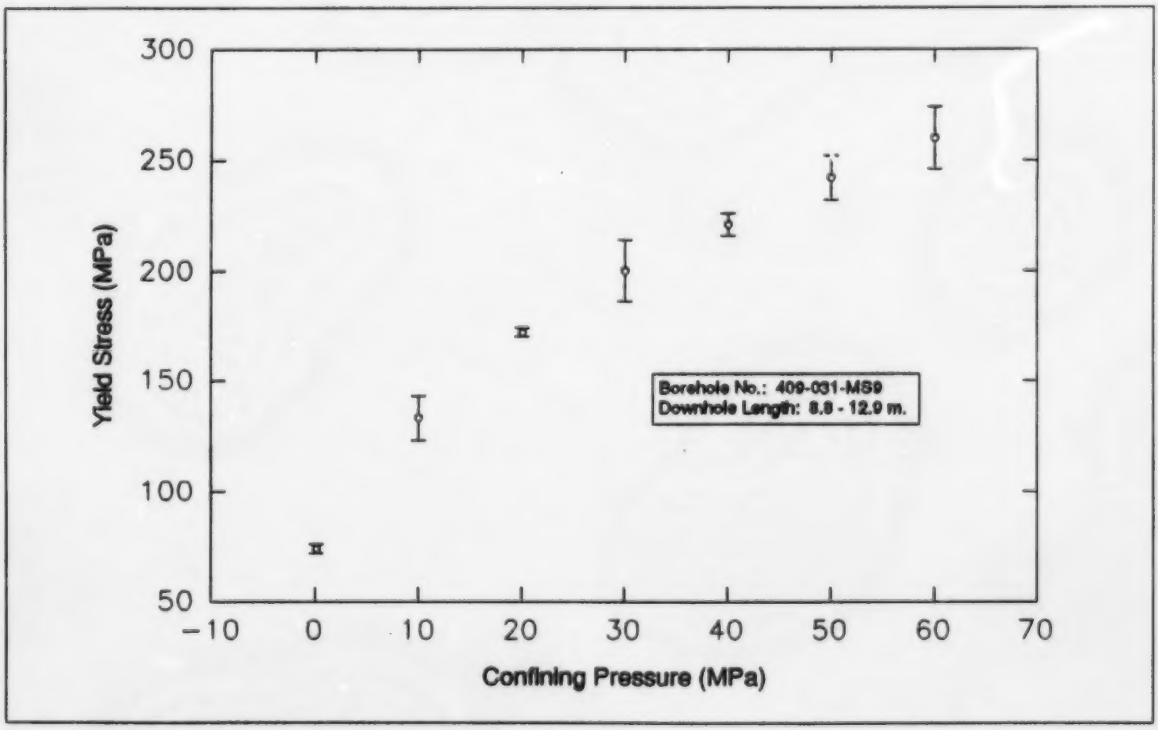

Figure 2 - Dilational Stress versus Confining Pressure

$$m = \frac{1}{\sigma_c}\left[\frac{\Sigma x_i y_i - \frac{\Sigma x_i \Sigma y_i}{n}}{\Sigma x_i^2 - \frac{(\Sigma x_i)^2}{n}}\right] \tag{4}$$

where $x = \sigma_3$

$y = (\sigma_1 - \sigma_3)^2$

n = total number of data pairs x_i and y_i

The coefficient of determination r^2 is given by:

$$r^2 = \frac{\left[\Sigma x_i y_i - \frac{\Sigma x_i \Sigma y_i}{n}\right]^2}{\left[\Sigma x_i^2 - \frac{(\Sigma x_i)^2}{n}\right]\left[\Sigma y_i^2 - \frac{(\Sigma y_i)^2}{n}\right]} \tag{5}$$

Hoek and Brown also suggest that the relationship between the normal and shear stresses (σ and τ) and the principal stresses at failure can be expressed as follows:

$$\sigma = \sigma_3 + \frac{\tau_m^2}{\tau_m + m\sigma_c/8} \tag{6}$$

$$\tau = (\sigma - \sigma_3)\sqrt{1 + m\sigma_c/4\tau_m} \tag{7}$$

where $\tau_m = \frac{1}{2}(\sigma_1 - \sigma_3)$

By substituting successive pairs of σ_1 and σ_3 into Equations 9 and 10, a Mohr failure envelope can be generated.

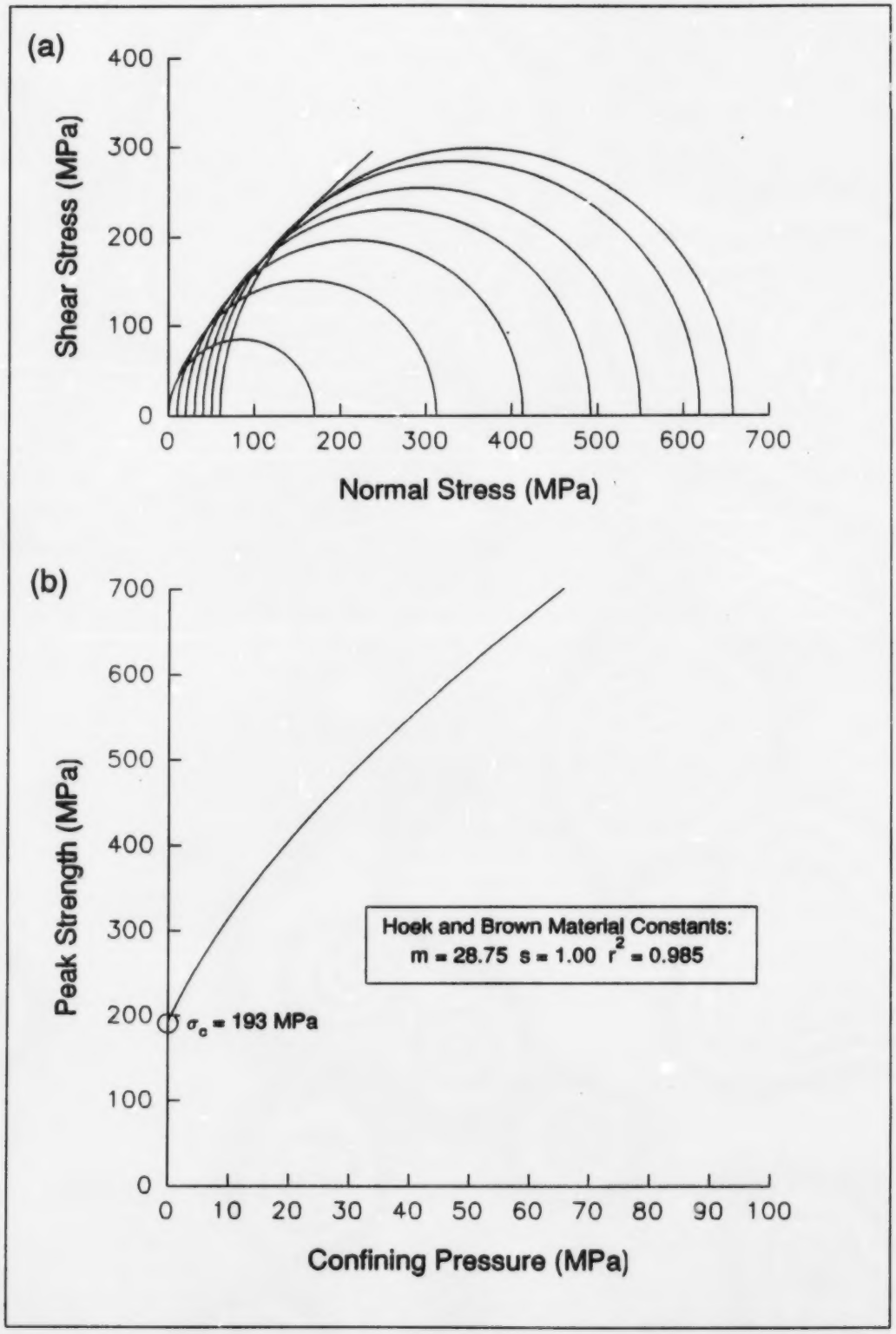

Figure 3 - Mohr-Coulomb and Hoek and Brown Failure Criteria Analyses, Peak Deviator Stress

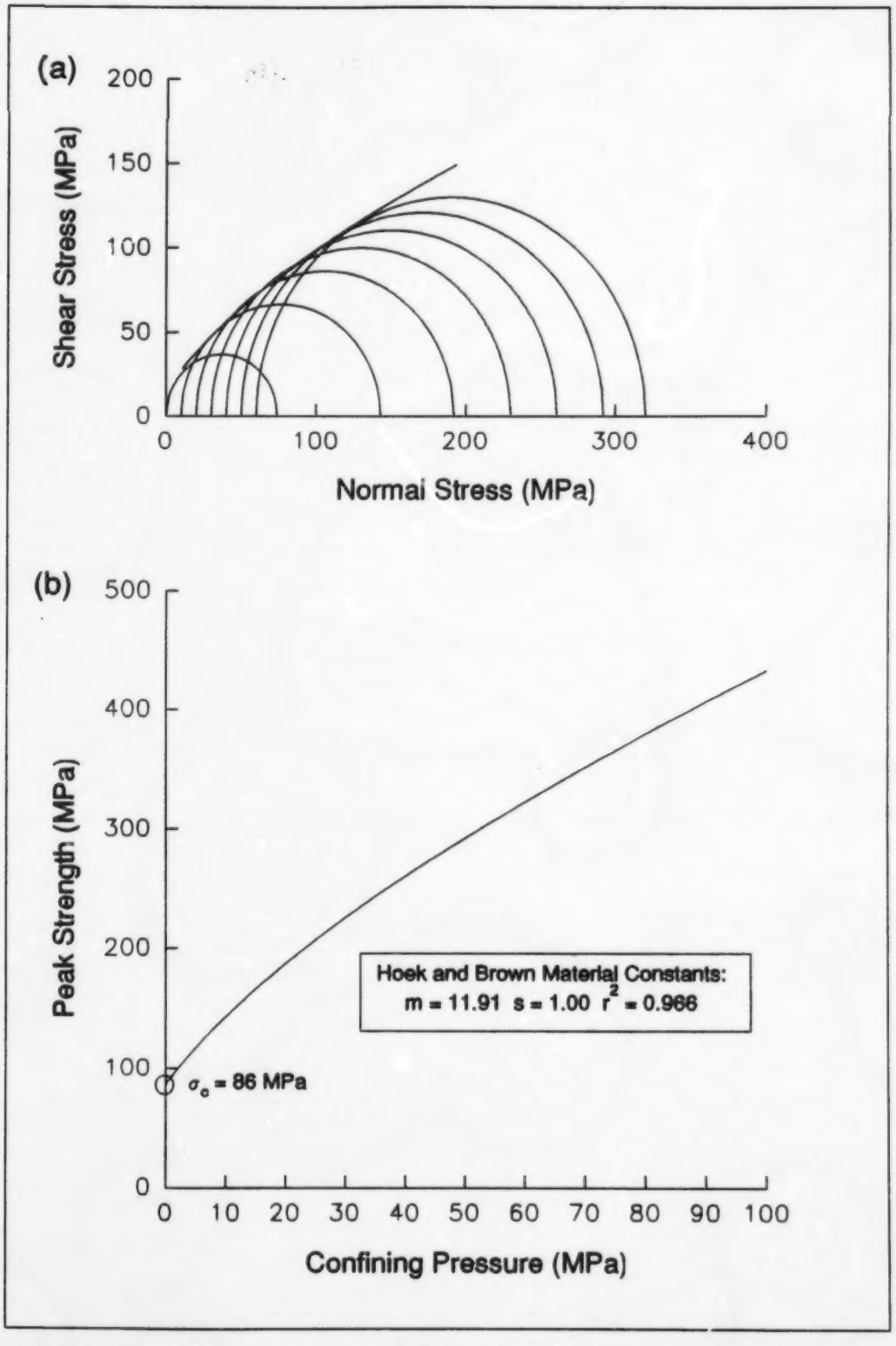

Figure 4 - Mohr-Coulomb and Hoek and Brown Failure Criteria Analyses, Dilational Stress

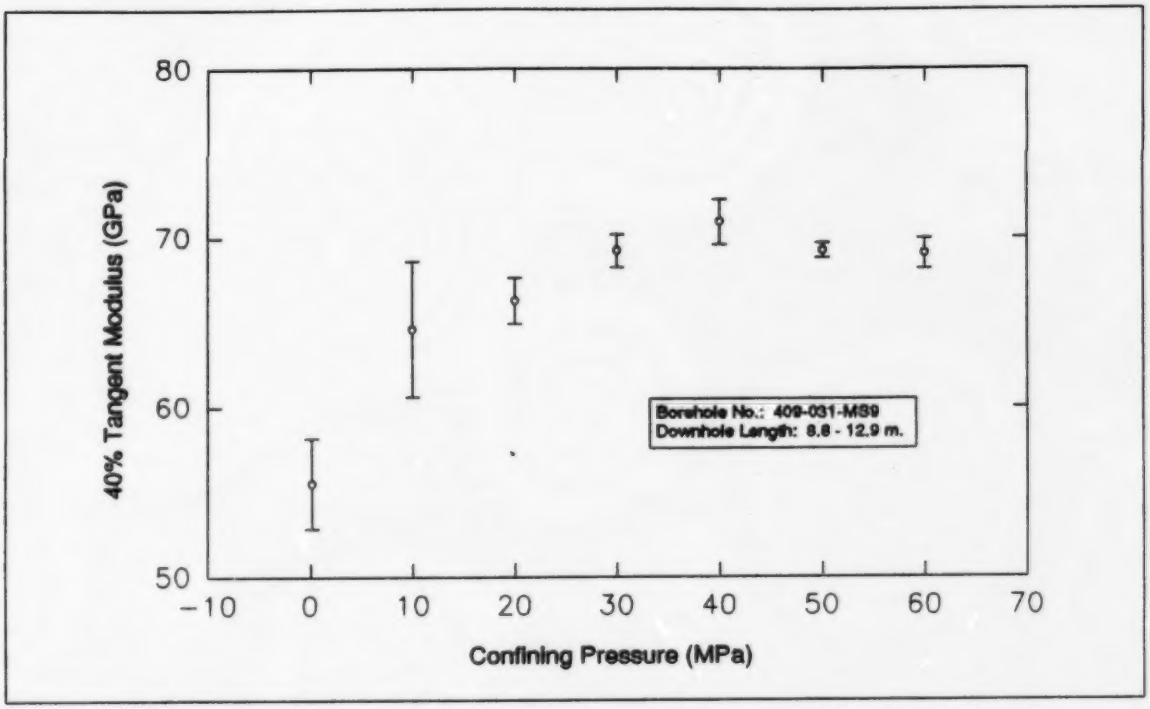

Figure 5 - 40% Tangent Modulus versus Confining Pressure

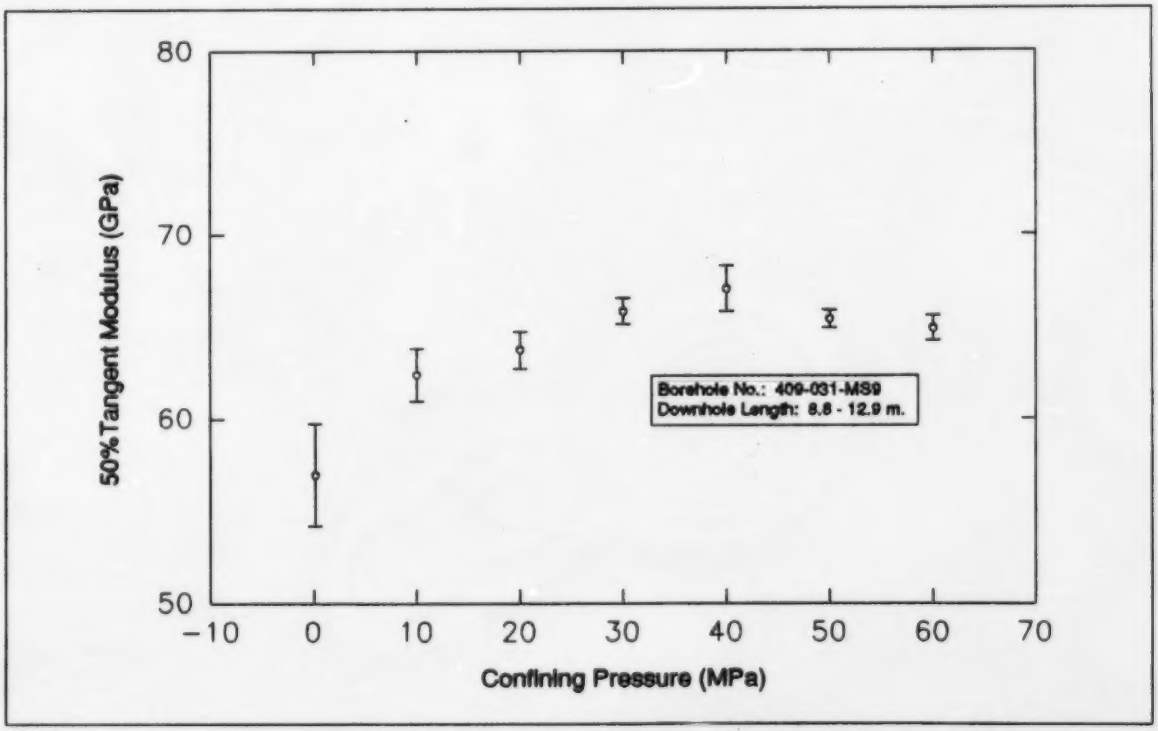

Figure 6 - 50% Tangent Modulus versus Confining Pressure

Figure 3a illustrates the Mohr circles generated using the mean peak deviator stresses determined for each confining pressure increment used for this test program. The failure envelope also shown in the figure was cinstructed using the Hoek and Brown analyses and shows a good fit to the observed data. Figure 3b provides a summary of the peak strengths also predicted using the Hoek and Brown analyses. As the figure indicates, an m value of 28.75, r^2 of 0.985 and σ_c of 193 MPa were calculated from the peak deviator stresses of the individual specimens.

Figure 4 provides the same analyses found in Figure 3 conducted, however, on the dilational strengths determined using the deviation from linear-elastic vometric strain method. Again, Figure 4a indicates a good fit between the failure envelopes predicted using the Hoek and Brown and Mohr-Coulomb analyses. The dilational strength m value was calculated as 11.91 with a coefficient of determination, r^2, of 0.966 and a predicted uniaxial compressive strength equal to 86 MPa.

Tangent Modulus of Elasticity

Typical laboratory scale characterization of rock includes an estimate of the 50% tangent modulus of elasticity presumably because it is representative of the linear-elastic behaviour of the rock type in question. Deviation from linear-elastic volumetric strain analyses done as part of this study, however, shows that new crack formation for this rock type begins at approximately 43% of the peak deviator stress. Data was, consequently, reanalysed to determine the 40% tangent modulus of elasticity. As Table 4 and Figures 5 and 6 indicate, with the exception of uniaxial results, the 40% tangent modulus was consistently higher than those determined at 50% of the peak deviator stress. This would imply that the specimen is more intact at the lower stress level and has, indeed, begun to show new crack formation if not failure at 50% of the peak deviator stress.

Both moduli increase with the application of successively higher confining pressures up to σ_3 equal to approximately 30 MPa. After this point, the 40% modulus tends to plateau out at a value of approximately 69.62 GPa (σ^2 = 0.87 GPa) while the mean 50% modulus in this region (30 MPa < σ_3 < 60 MPa) was 65.80 GPa (σ^2 = 0.91 GPa).

Poisson's Ratio

For the reasons outlined above, Poisson's ratios were also determined at stress levels equal to 40% (ν_{40}) and 50% (ν_{50}) of the peak deviator stress. As Table 4 indicates and Figures 7 and 8 graphically illustrate, the Poisson's ratios determined at 40% ($\bar{\nu}_{40}$=0.33) of the peak deviator stress are consistently lower than those determined at 50% ($\bar{\nu}_{50}$=0.41).

While some increase in axial Young's modulus was observed as the reference stress level was decreased from 50% to 40% of the peak deviator stress, that increase was insufficient to account for the 24% decrease in Poisson's ratio observed when comparing the two stress levels. It is, in fact, the much higher transverse moduli observed at 40% of (σ_1-σ_3) that govern the lower Poisson's ratios determined at that stress level. The transverse modulus is particularly sensitive to crack formation during axial loading since new cracks tend to form parallel to the loading direction. The resultant increase in transverse strain, results in a lower transverse modulus and, consequently, the higher Poisson's ratios observed at the 50% stress level.

As Figure 8 illustrates, the mean 50% Poisson's ratios show a tendency to decrease as the confining pressure increases from 20 MPa to 60 MPa. This would tend to indicate that the increasing confining pressure is preventing or, at least, retarding the initiation, propagation or opening of new cracks. Even at σ_3=60 MPa, however, the mean observed Poisson's ratio of 0.38 is 18% higher than the mean value of the 40% Poisson's ratio which, incidently, showed little variation over the entire confining pressure range used for testing. This serves as further evidence that signifigant new crack growth has begun at stress levels as low as 50% of the peak deviator stress.

Conclusions and Recommendations

In terms of the peak deviator stress, the samples obtained from borehole 409-031-MS9 exhibited the kind of behaviour which is usually anticipated for this type of rock, ie. increasing strength with increasing confining pressure. The deviation from linear-elastic volumetric strain method of analyses has, however, shed some interesting light on the pre-failure behaviour of the rock.

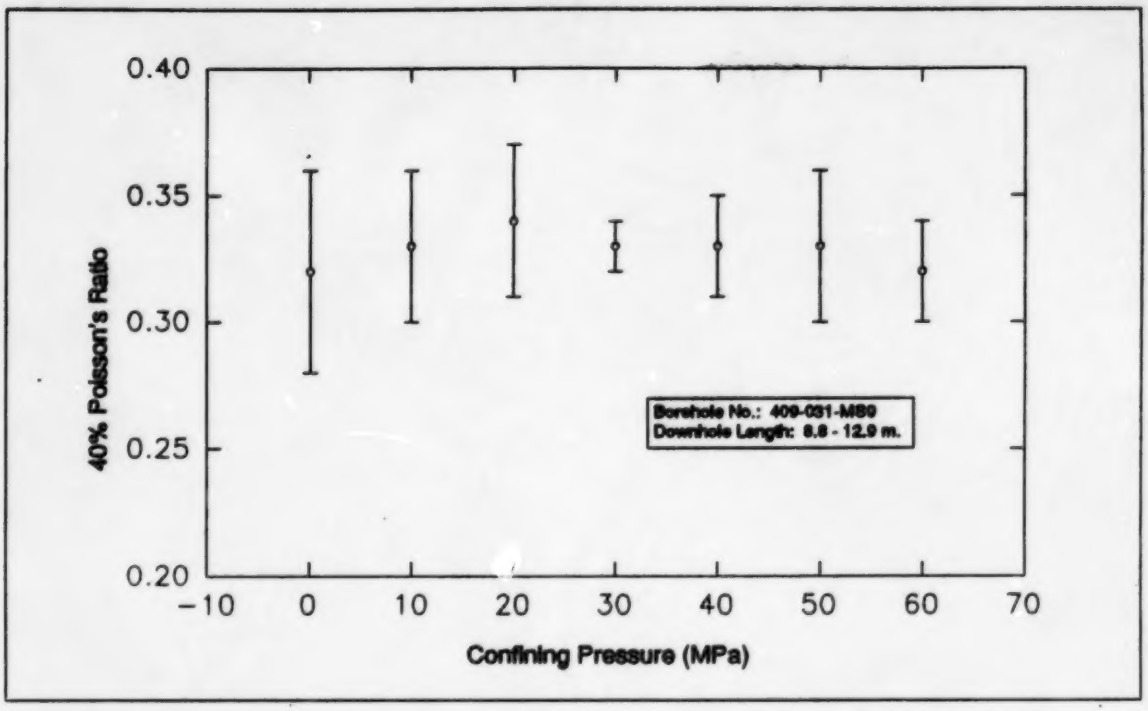

Figure 7 - 40% Poisson's Ratio versus Confining Pressure

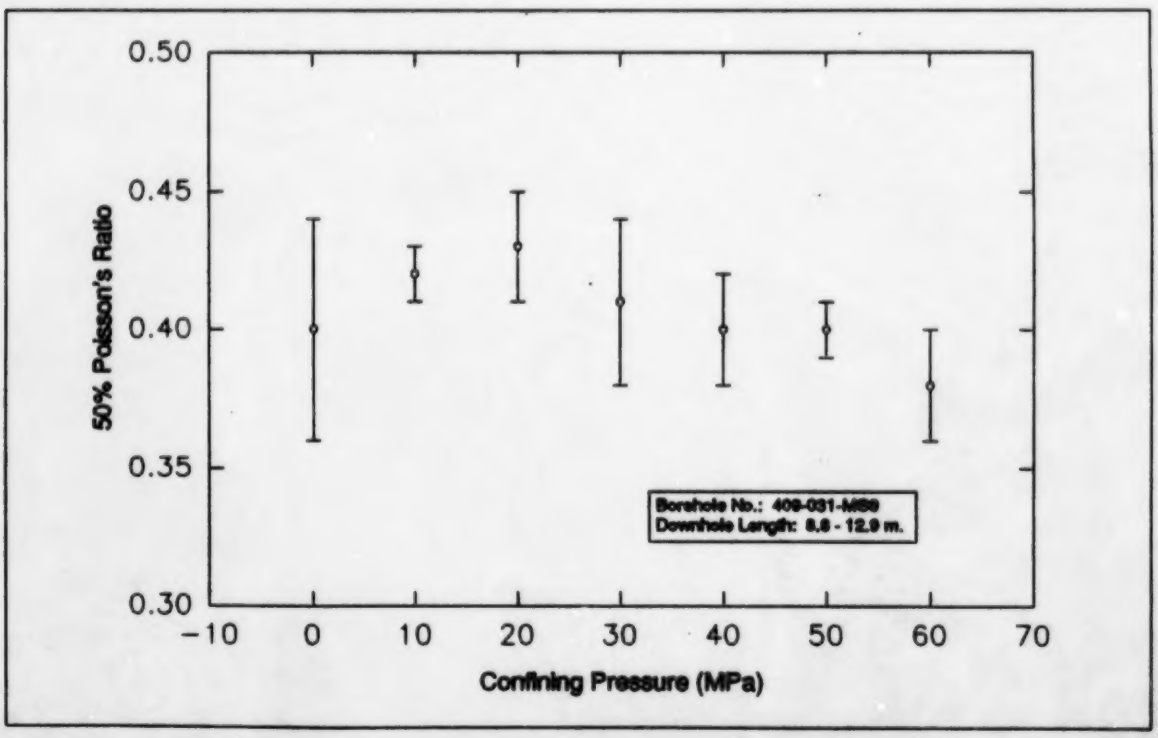

Figure 8 - 50% Poisson's Ratio versus Confining Pressure

It seems apparent from the comparison of the tangent modulus and Poisson's ratio data determined at 40% and 50% of the peak deviator stress that new crack initiation and propagation has begun before the 50% stress level has been reached. In fact, for this rock type, crack initiation appears to begin at approximately 43% of the peak deviator stress regardless of the level of confinement. It is a matter for conjecture and further study, however, as to whether or not the 43% stress level represents the long-term strength of the rock.

Acknowledgements

The author wishes to express his thanks to G. Larocque of CANMET for reviewing this report and making several helpful suggestions. Gratitude is expressed to J. Folta of CANMET, and Irene Muller and Robin Down, co-op students from the University of Waterloo, for the preparation of specimens and B. Gorski for carrying out the compression measurements.

References

Brown, E.T.; Rock characterization testing and monitoring, ISRM suggested methods'', International Society for Rock Mechanics, the Commission on Testing Methods, Pergamon, 211 p., 1981.

Gorski, B.; Post-failure uniaxial strength determinations using a servo-hydraulic test system'', Division Report MRL 87-33(INT), CANMET, Energy, Mines and Resources Canada, 77 p., 1987.

Gyenge, M. and Herget, G.; Pit slope manual supplement 3-2 - laboratory tests for design parameters'', CANMET Report 77-26, 74 p., 1977.

Gyenge, M. and Ladanyi, B.; Pit slope manual supplement 3-5 - sampling and specimen preparation'', CANMET Report 77-29, 30 p., 1977.

Hoek, E. and Brown, E.T.; Underground excavations in rock'', The Institution of Mining and Metallurgy, London, 527 p., 1980

MTS Systems Corporation; Operation manual for 815 rock mechanics test systems'', MTS Systems Corp., Minneapolis, Minnesota, U.S.A., 1986.

Simmons, G.R. and Soonawala, N.M.; Underground research laboratory experimental program'', Atomic Energy of Canada Limited Technical Record, TR-153, 126 p., 1982.

Simmons. G.R.; Operating phase experiments planned for Atomic Energy of Canada Limited's Underground Research Laboratory, Proc. International Symposium on Unique Underground Structures, vol. 2, 67-1:67-19, Denver, Colorado, U.S.A., 1990.

Vutukuri, V.S., Lama, R.D. and Saluja, S.S.; Mechanical properties of rocks, vol. 1, Transtech Publications, Clausthal, Germany, 26 p., 1974.

Appendix A

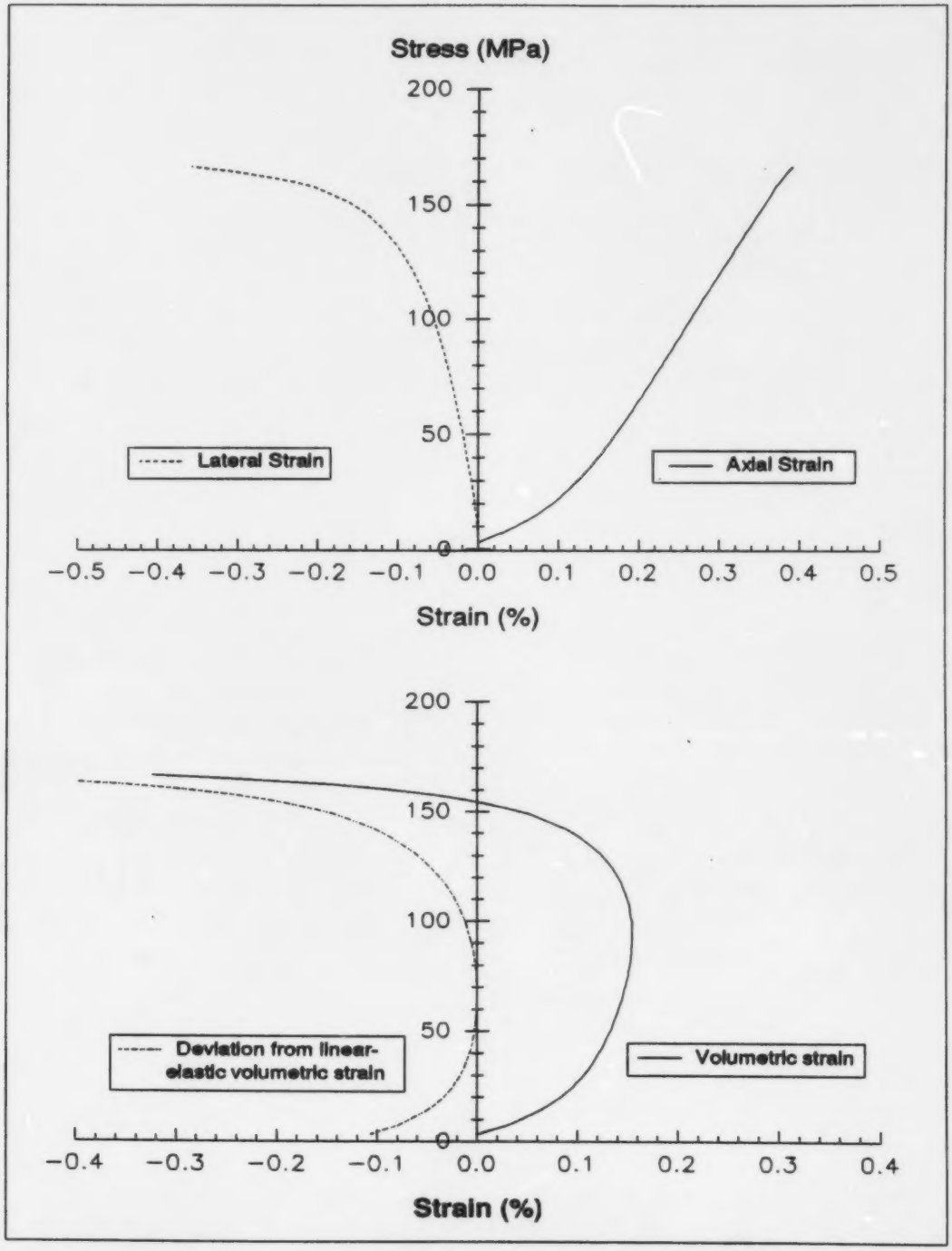

Figure A1 - Stress/strain curves for sample no. 8.800

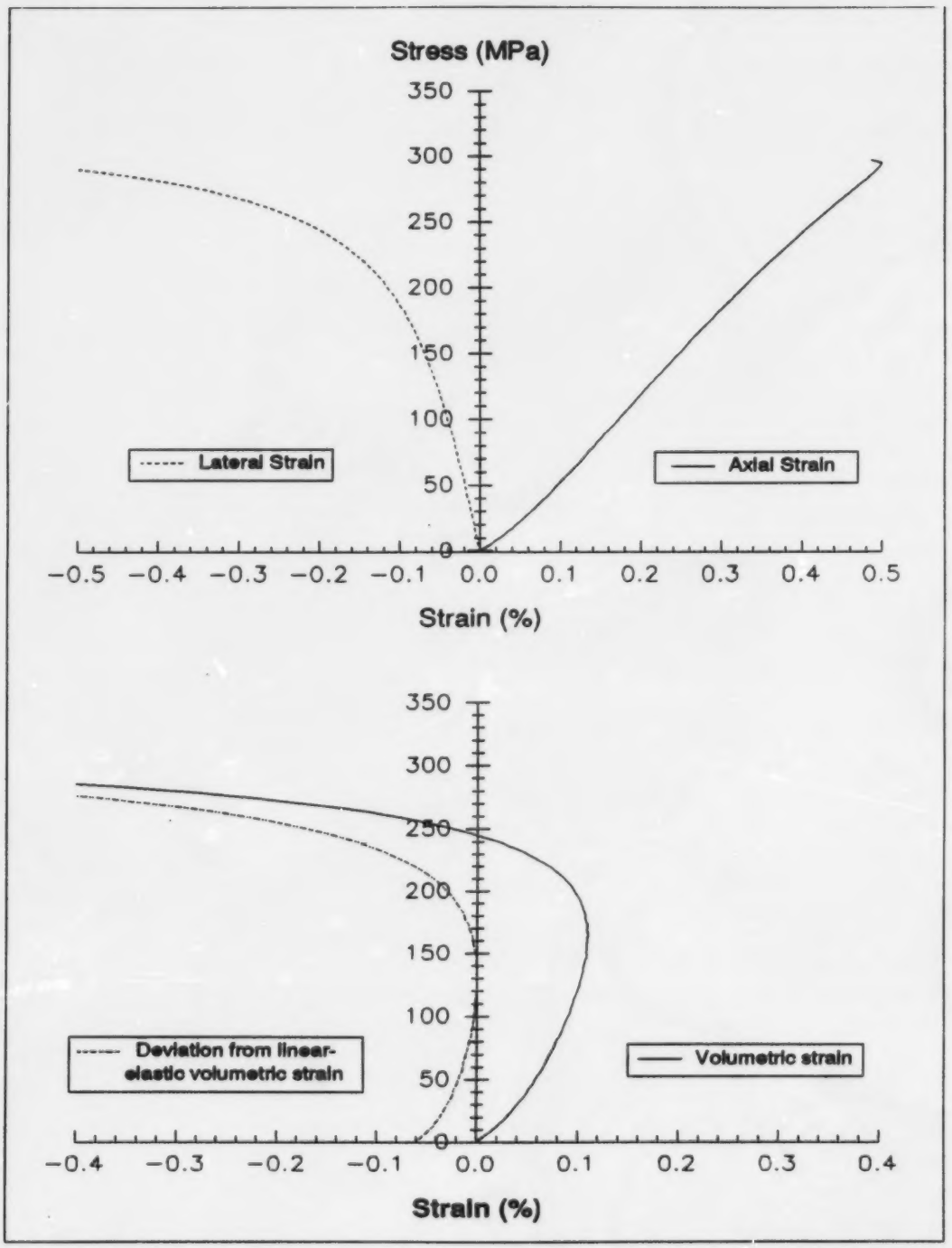

Figure A2 - Stress/strain curves for sample no. 8.900

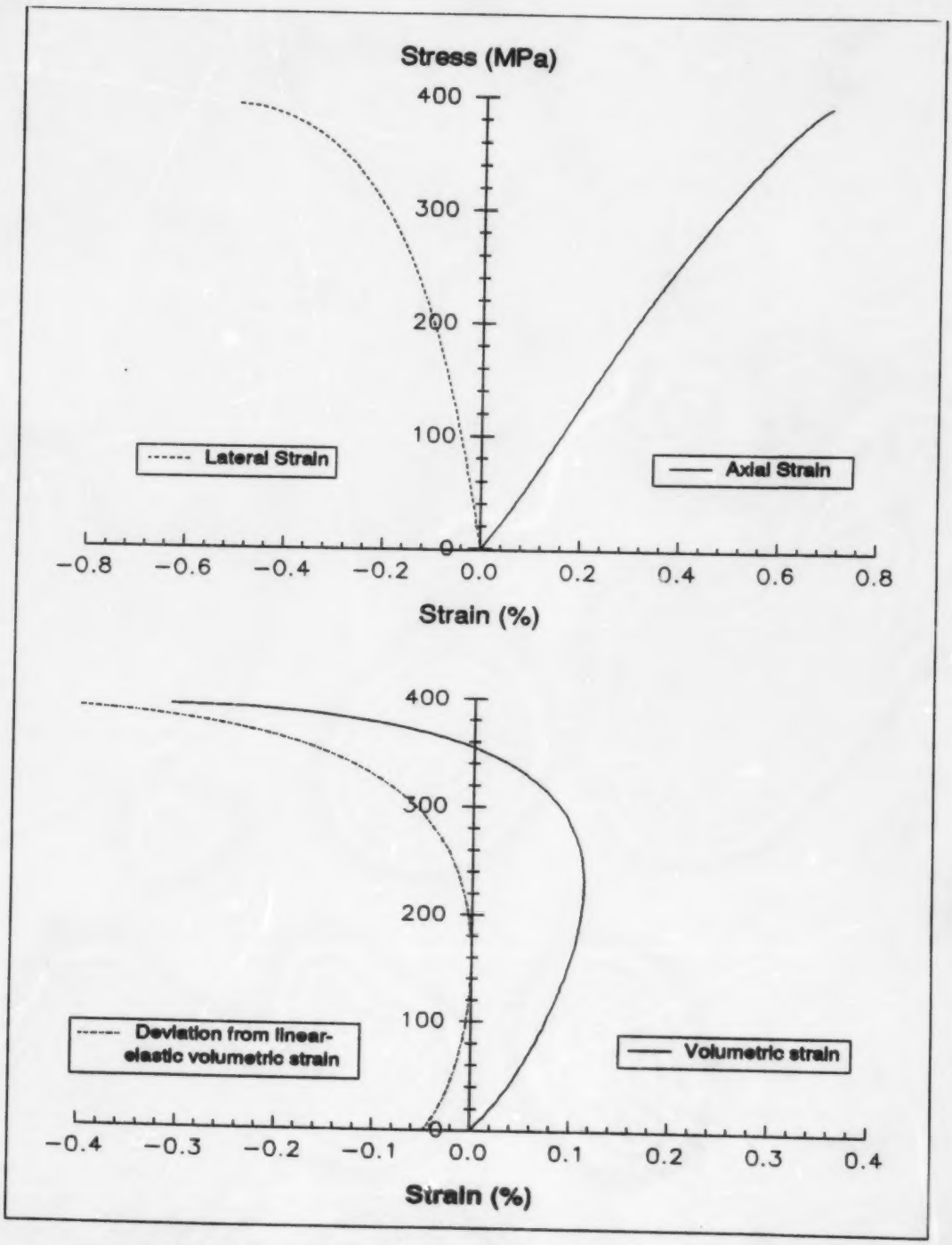

Figure A3 - Stress/strain curves for sample no. 9.077

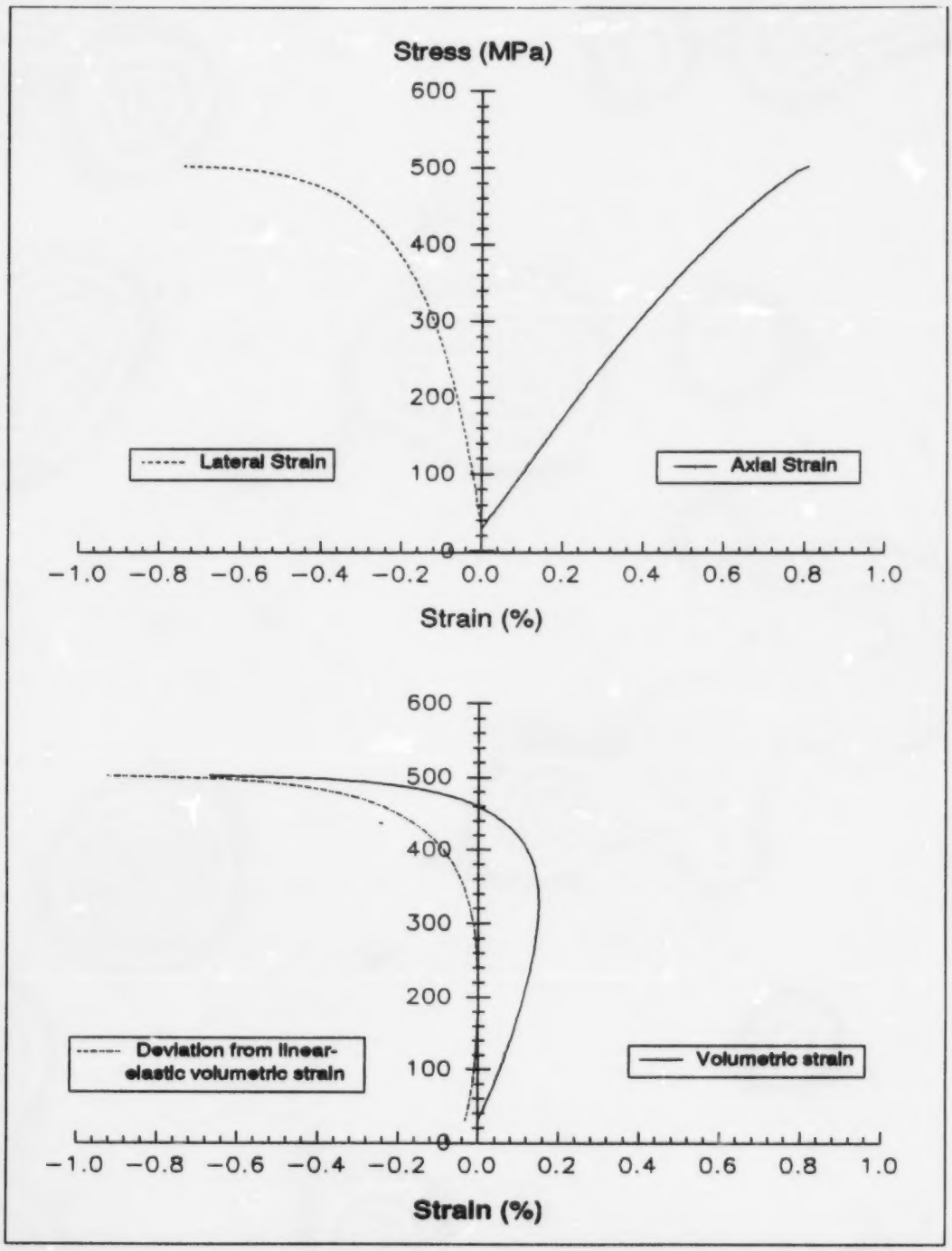

Figure A4 - Stress/strain curves for sample no. 9.185

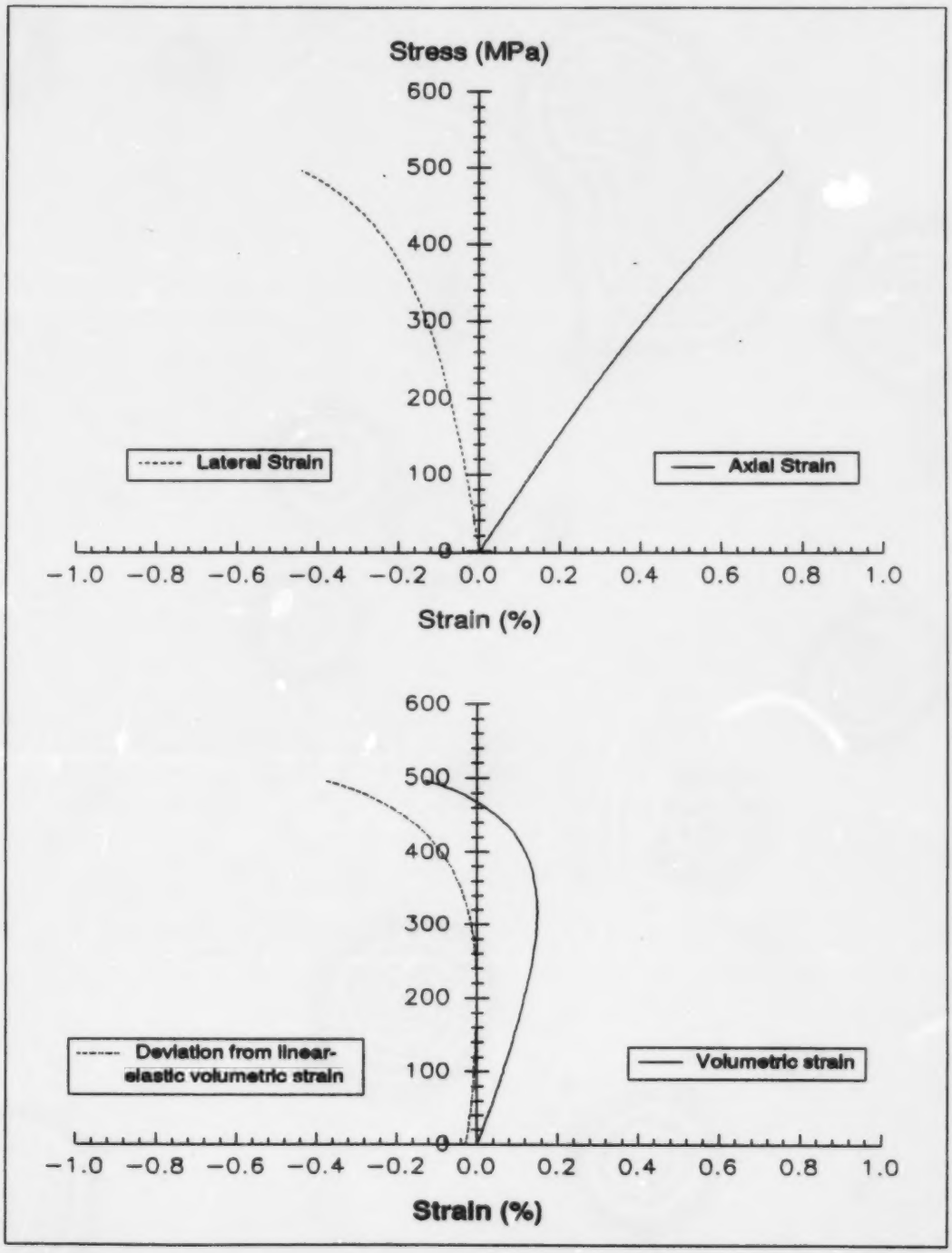

Figure A5 - Stress/strain curves for sample no. 9.369

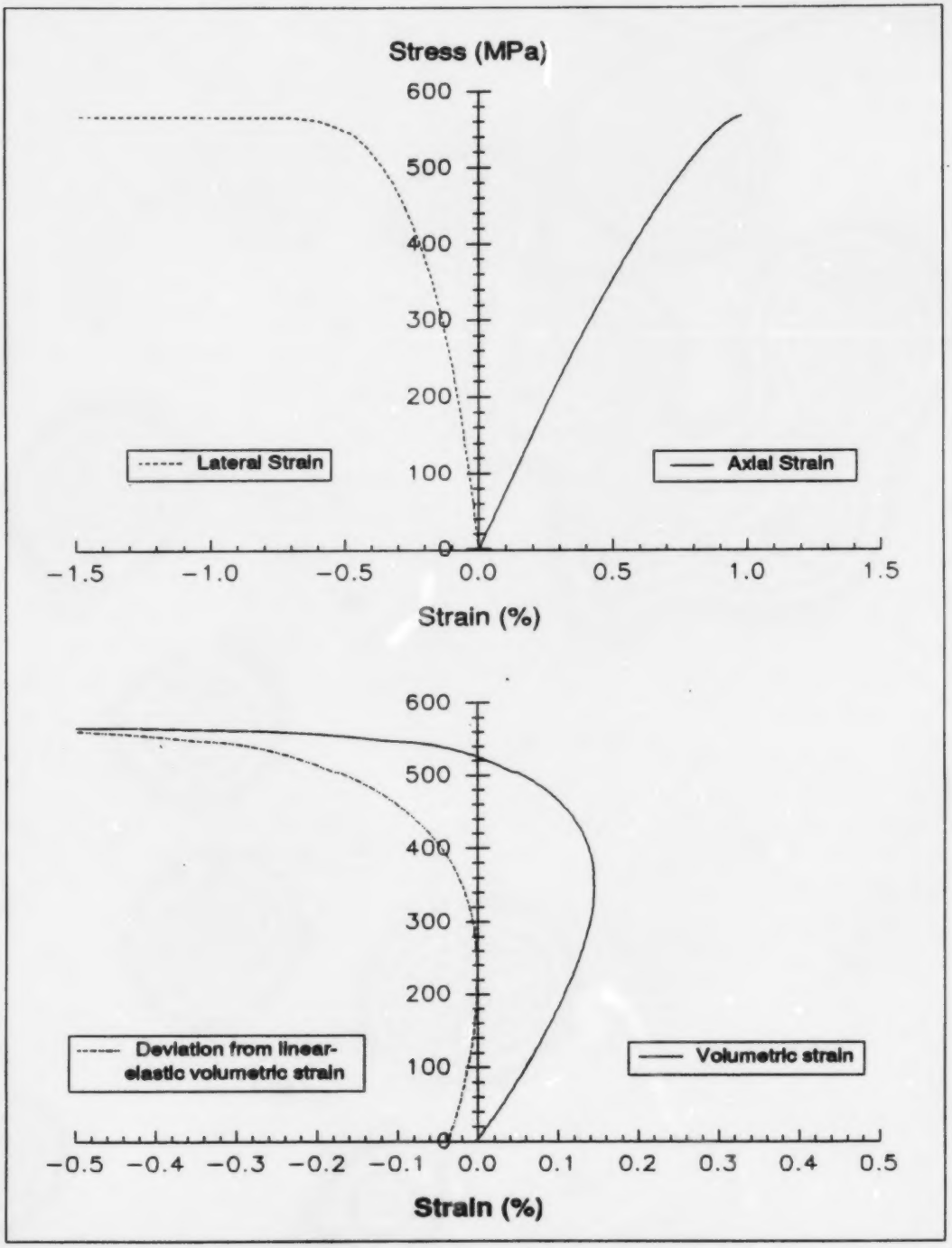

Figure A6 - Stress/strain curves for sample no. 9.475

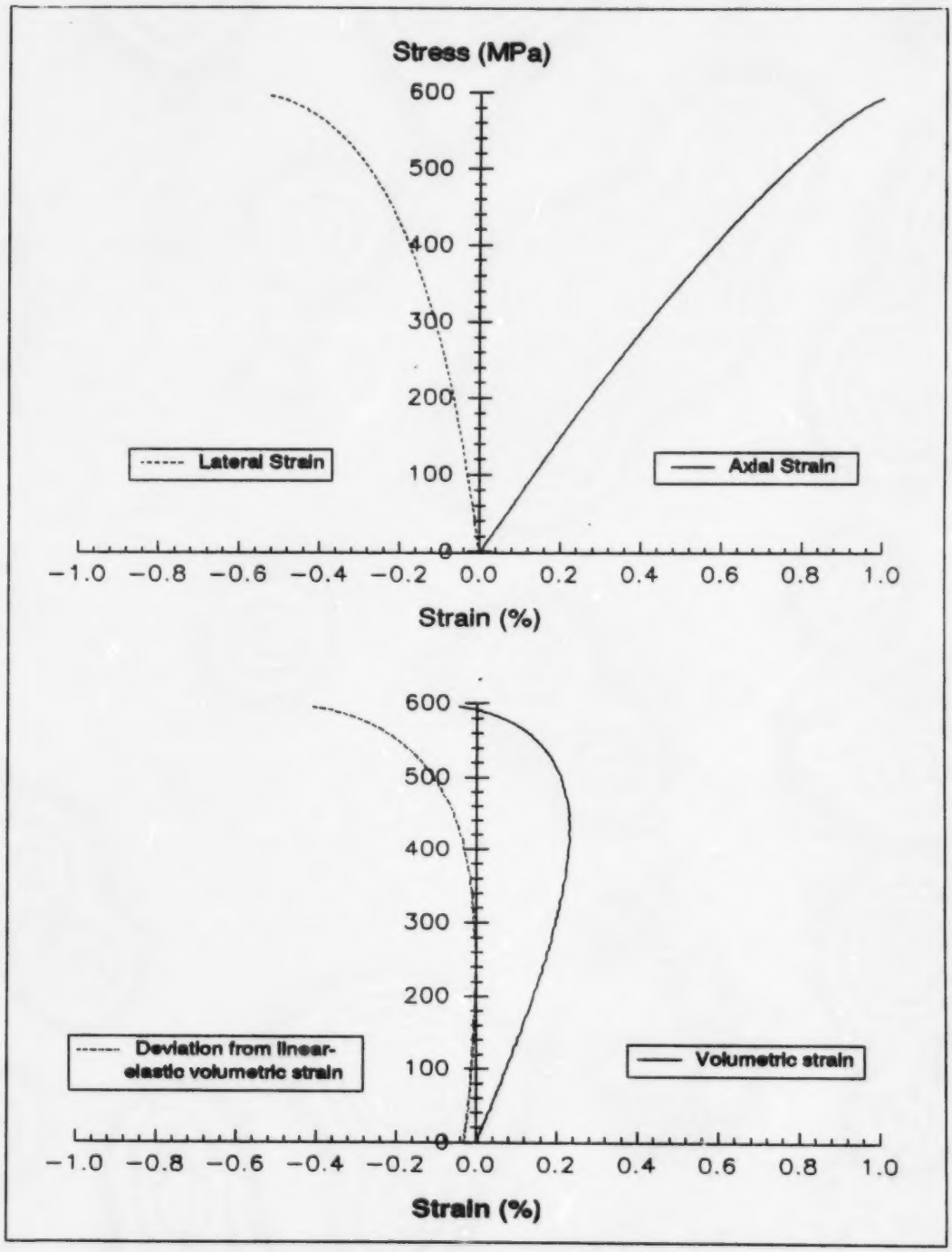

Figure A7 - Stress/strain curves for sample no. 9.581

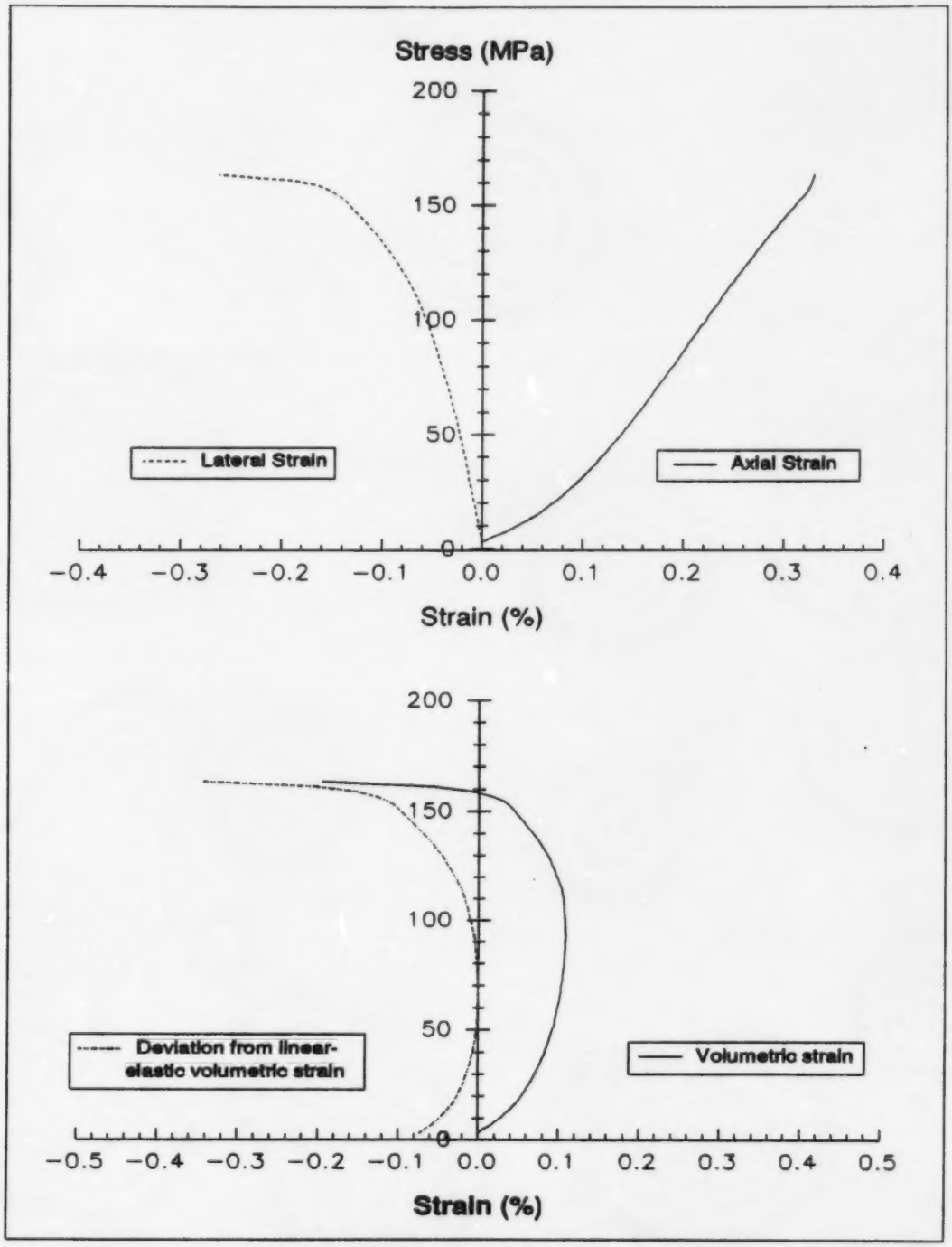

Figure A8 - Stress/strain curves for sample no. 9.720

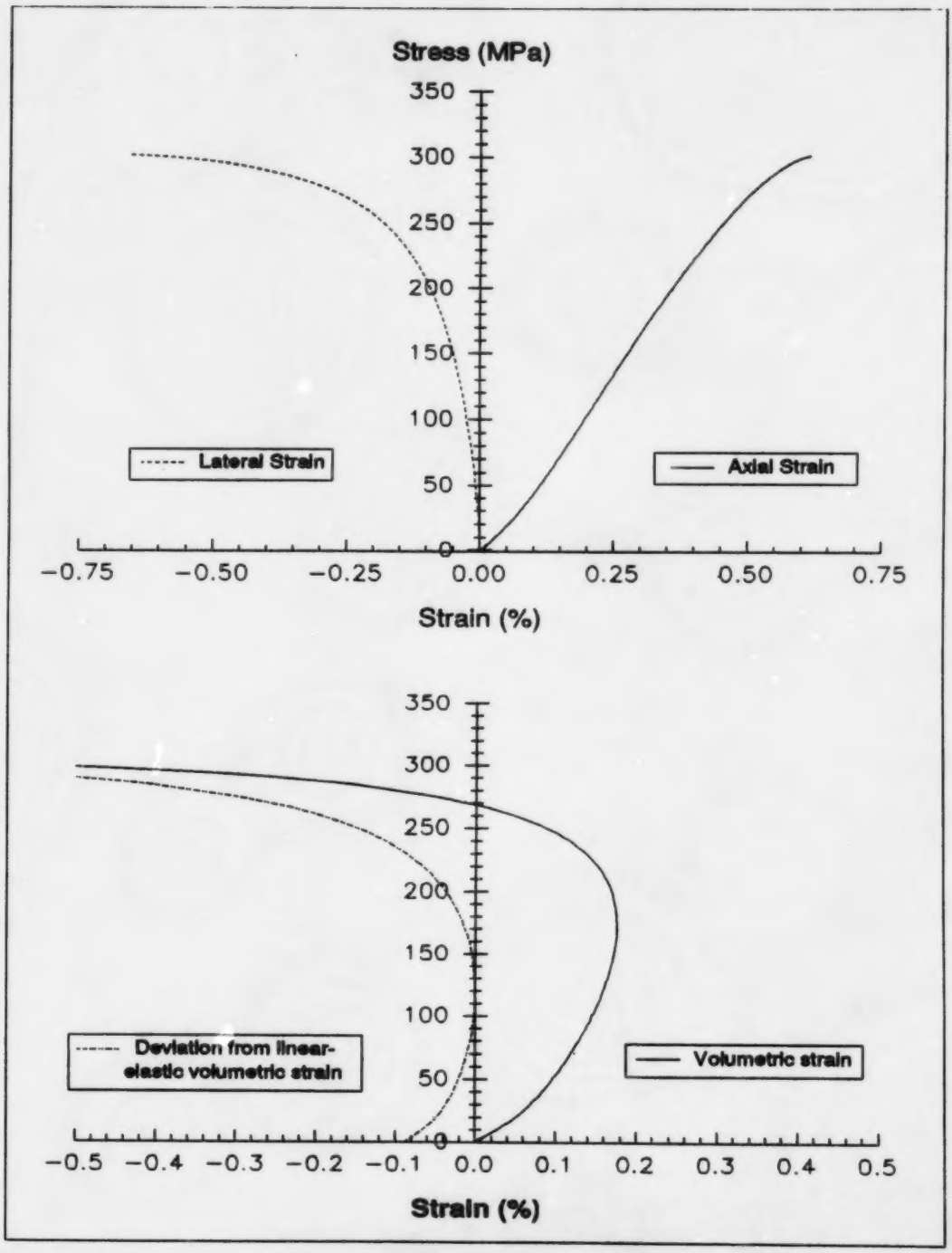

Figure A9 - Stress/strain curves for sample no. 9.827

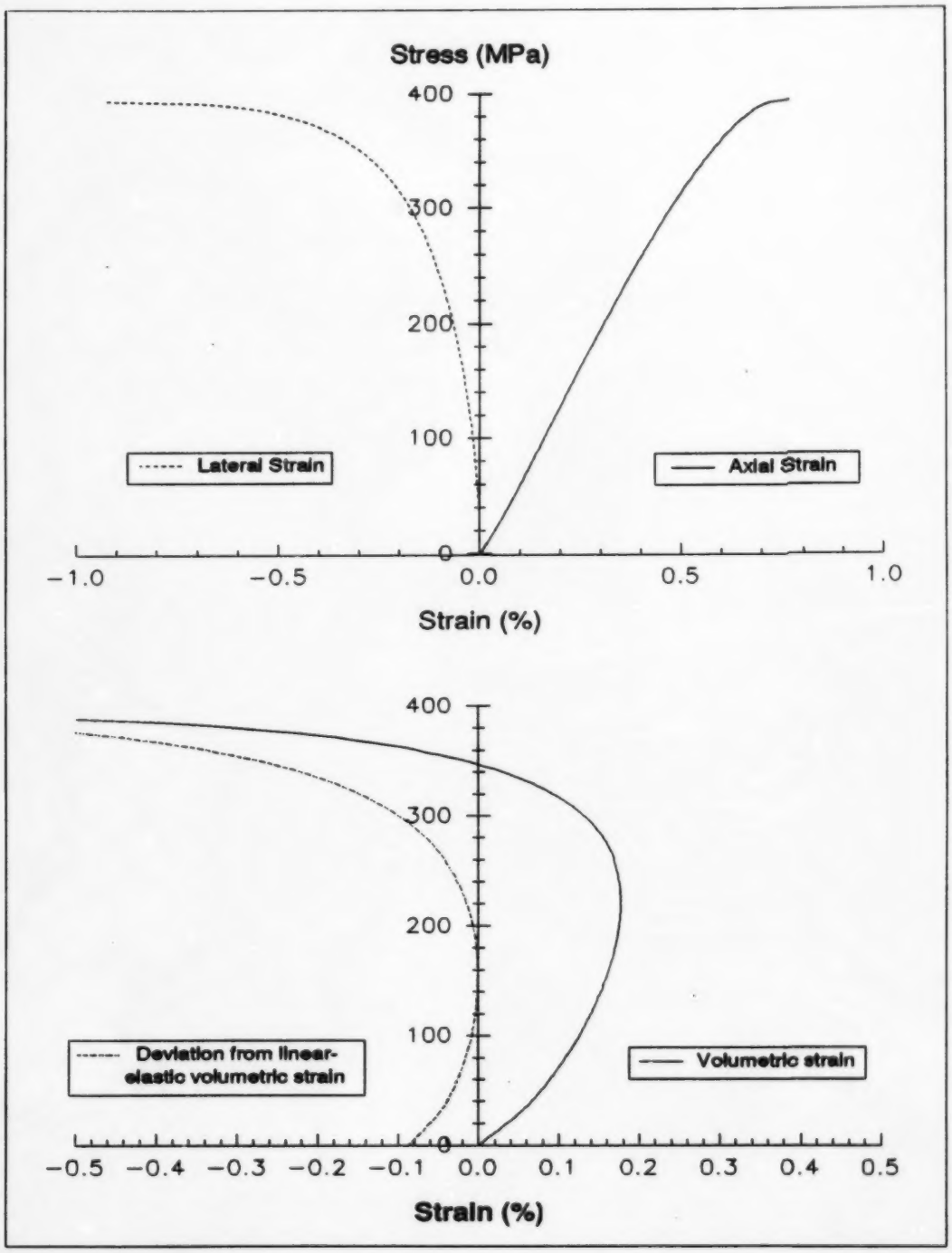

Figure A10 - Stress/strain curves for sample no. 9.933

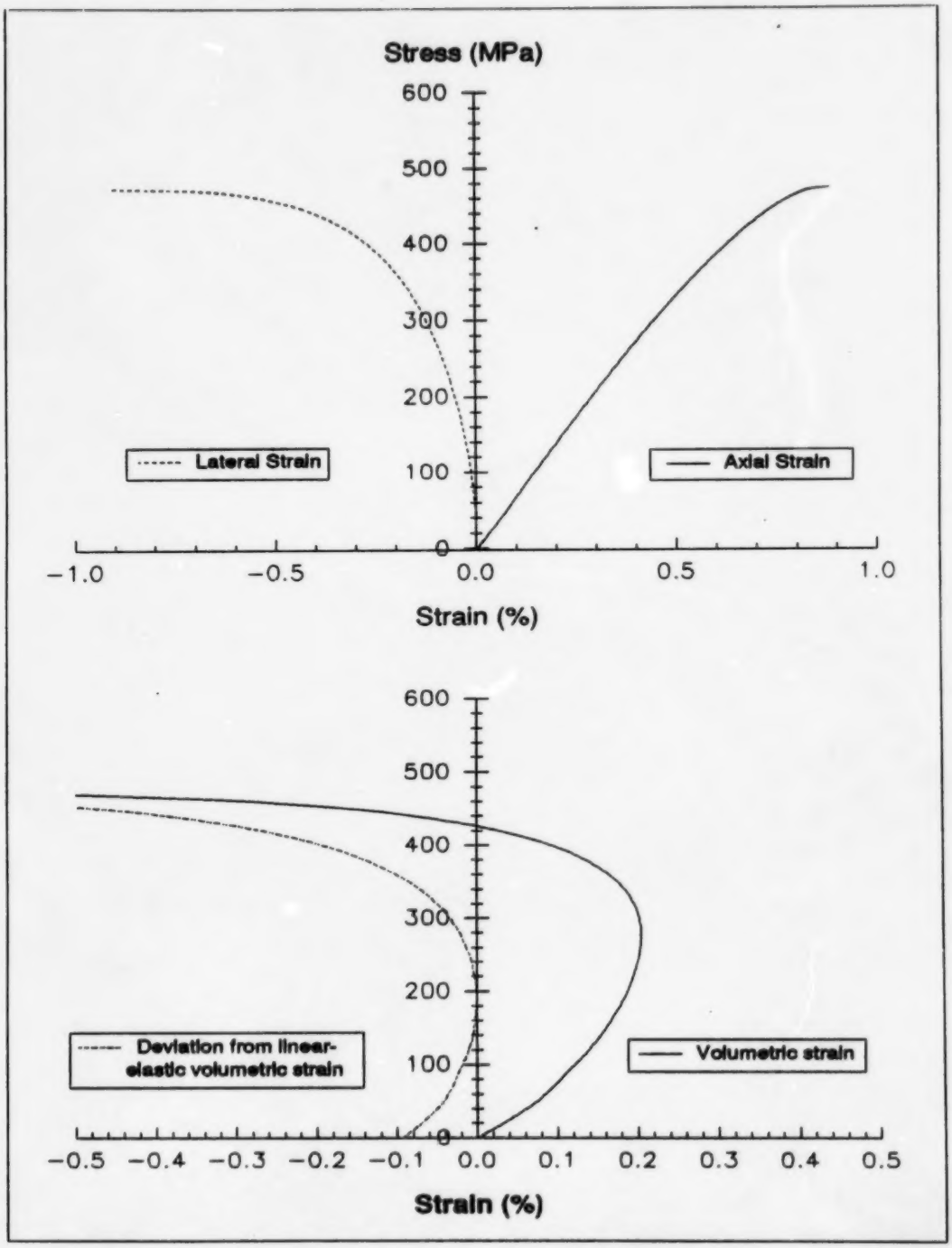

Figure A11 - Stress/strain curves for sample no. 10.142

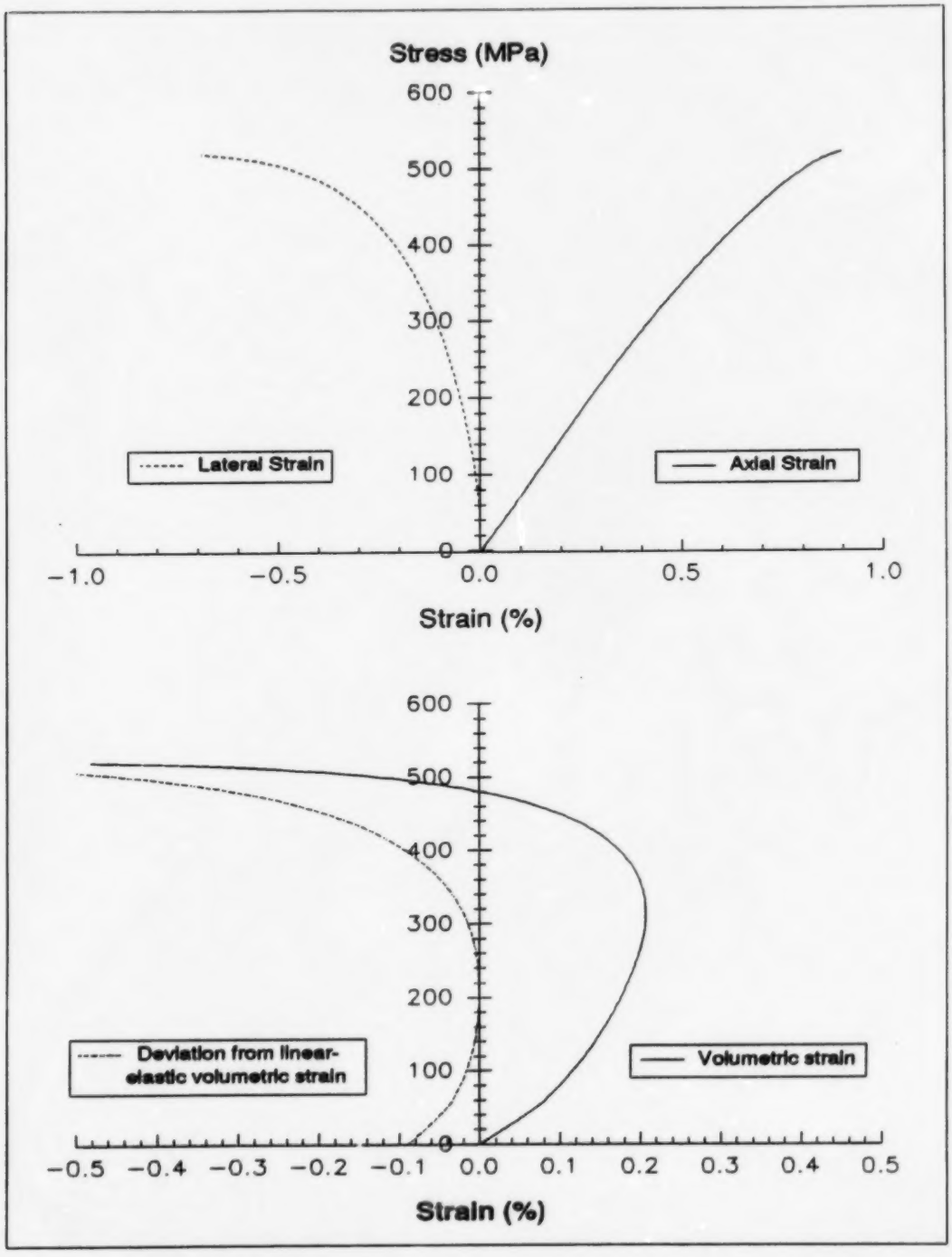

Figure A12 - Stress/strain curves for sample no. 10.250

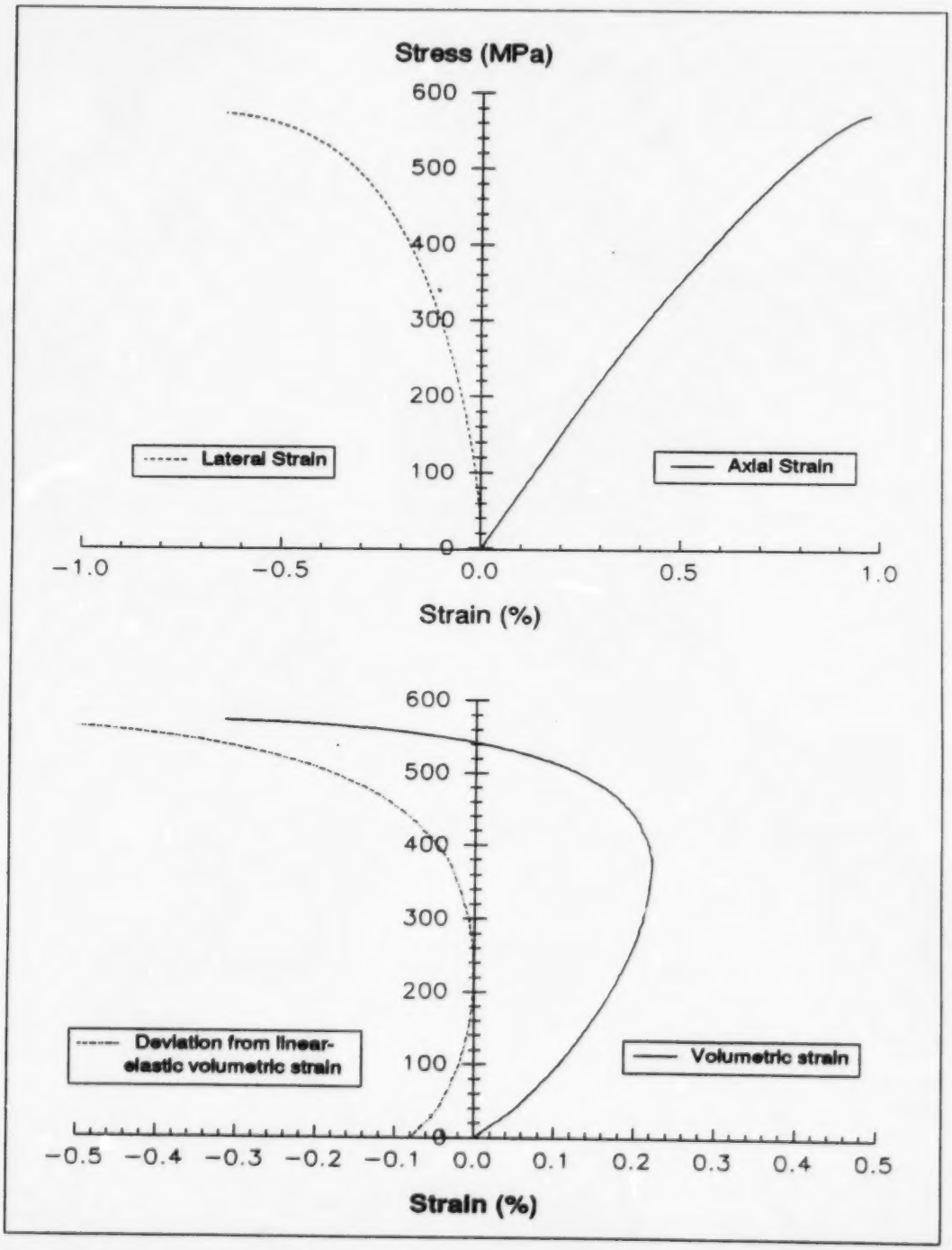

Figure A13 - Stress/strain curves for sample no. 10.386

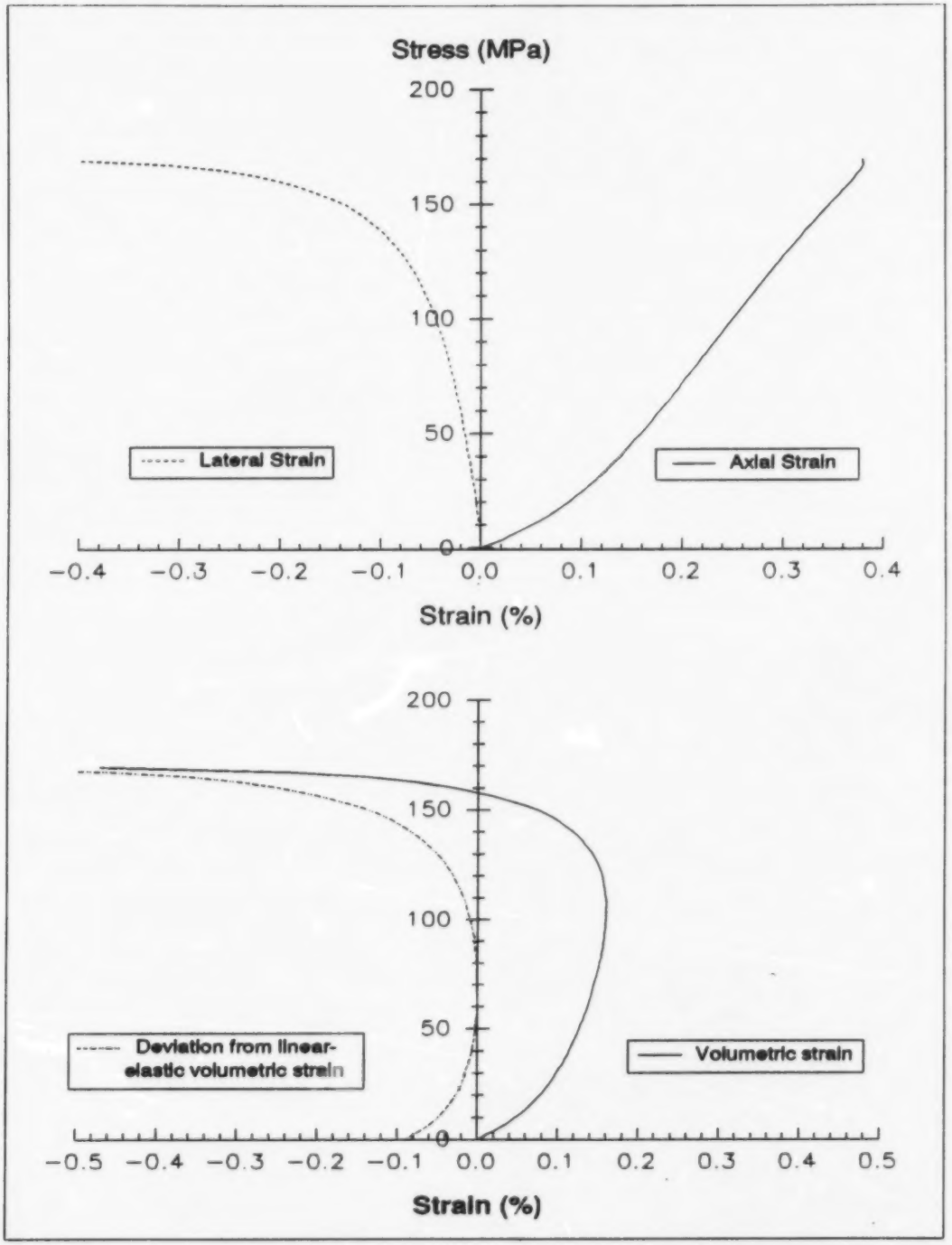

Figure A14 - Stress/strain curves for sample no. 10.598

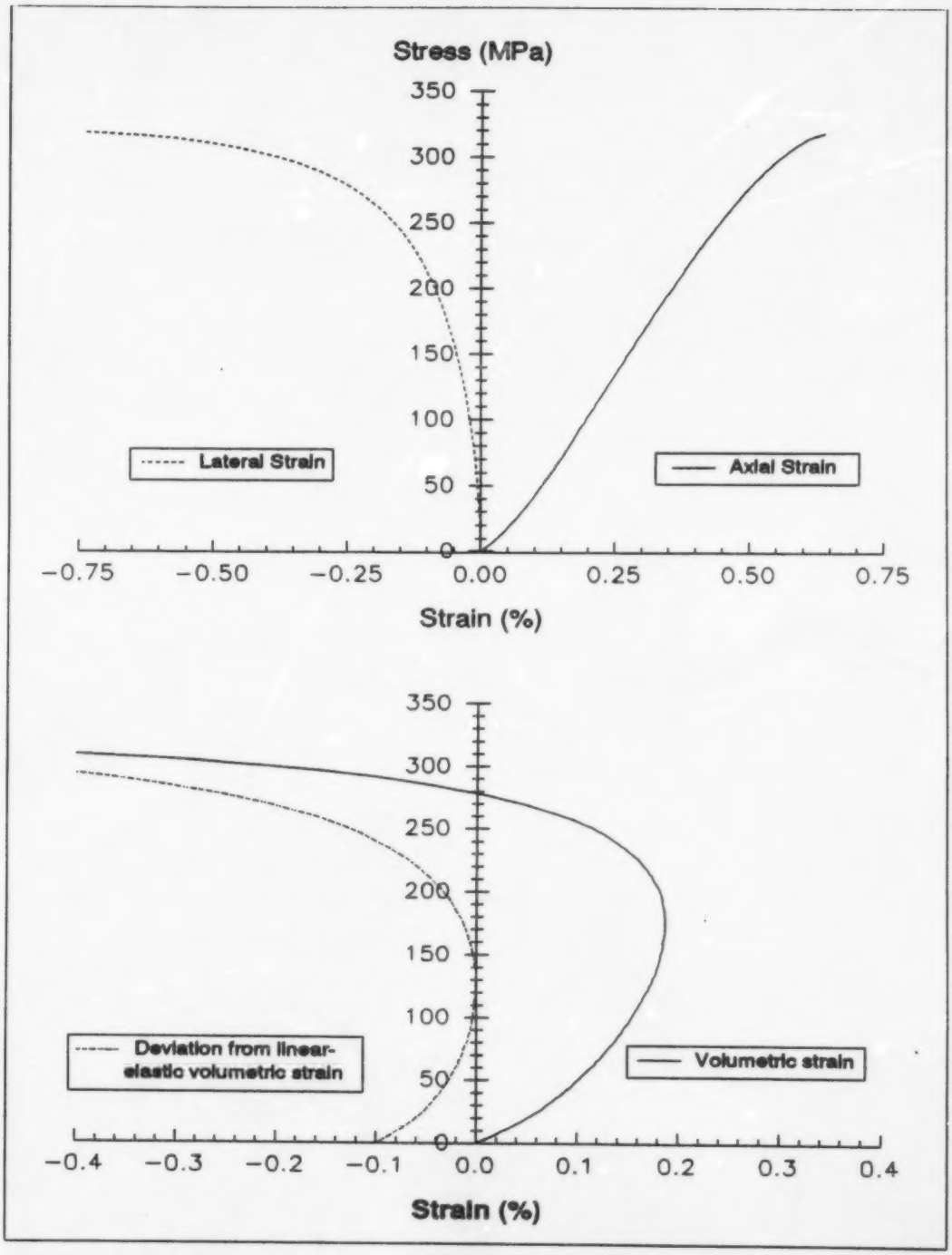

Figure A15 - Stress/strain curves for sample no. 10.705

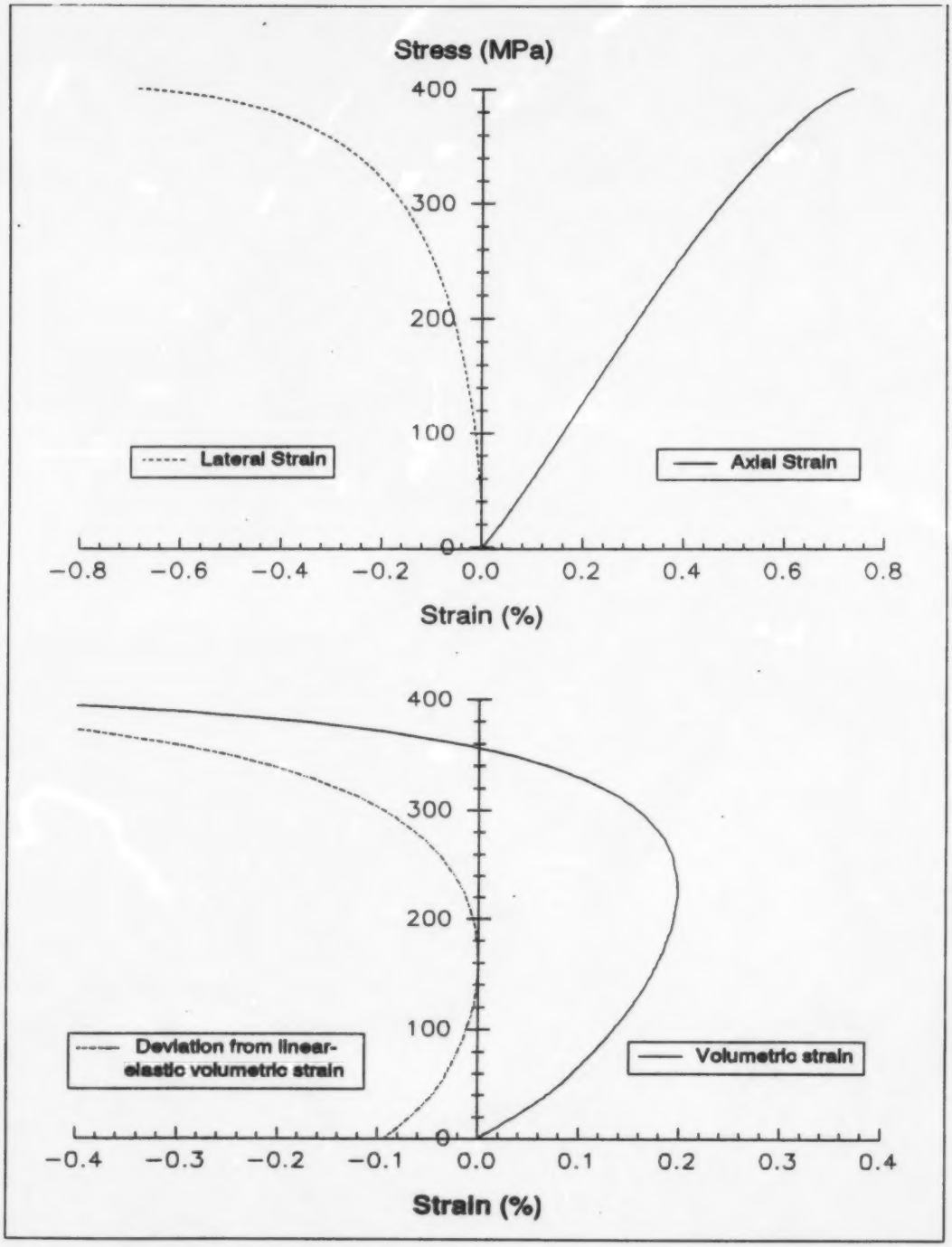

Figure A16 - Stress/strain curves for sample no. 11.040

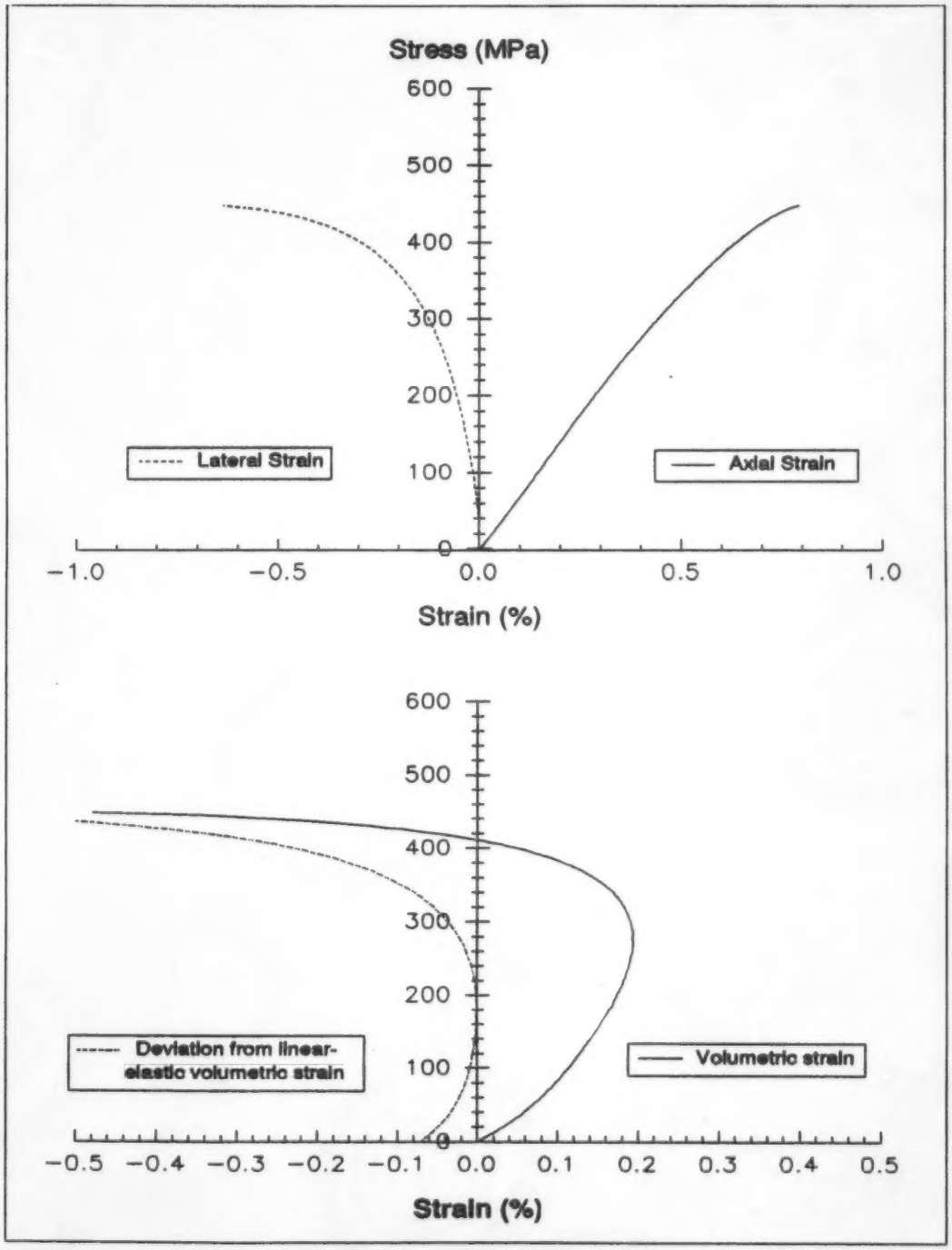

Figure A17: Stress/strain curves for sample no. 11.149

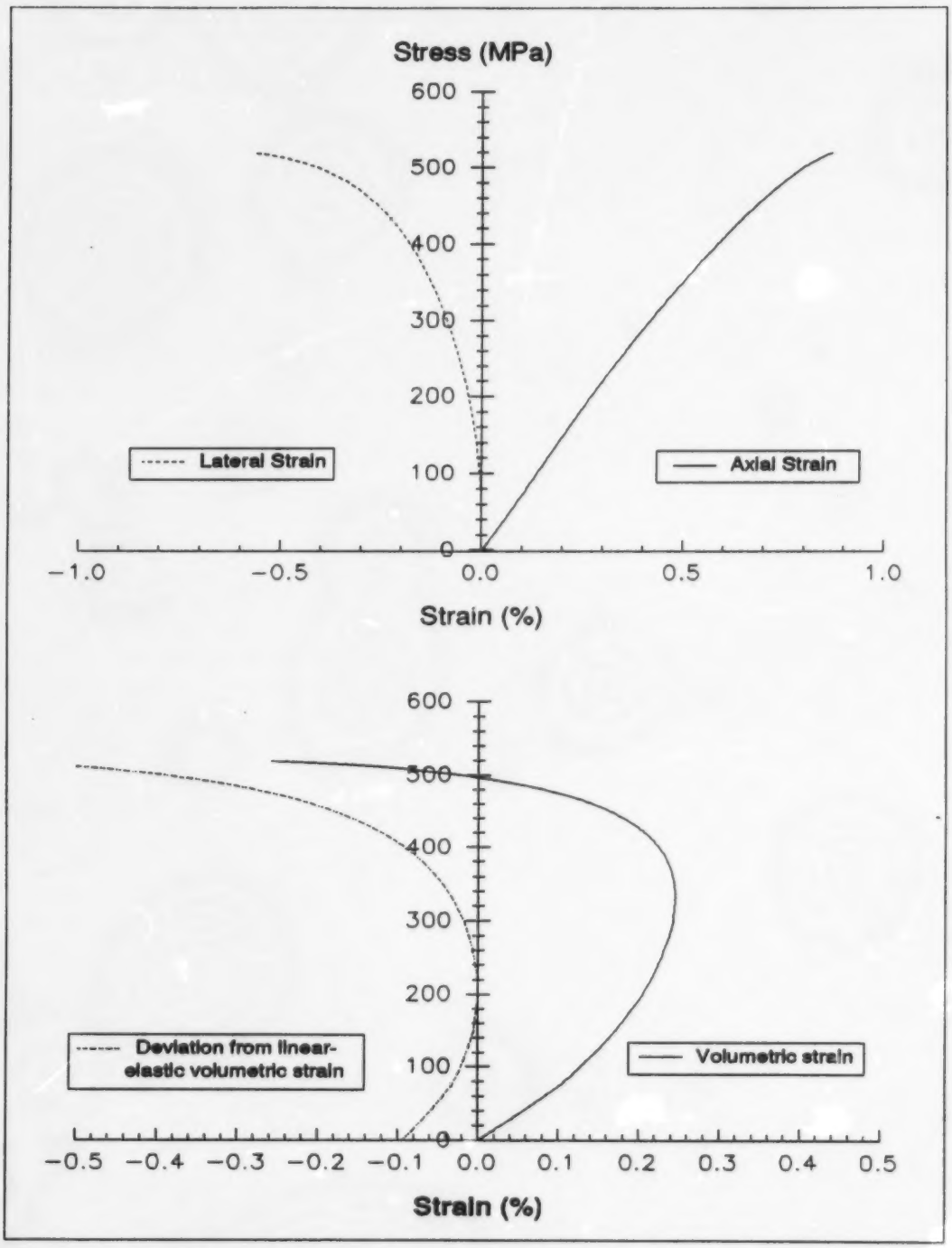

Figure A18 - Stress/strain curves for sample no. 11.257

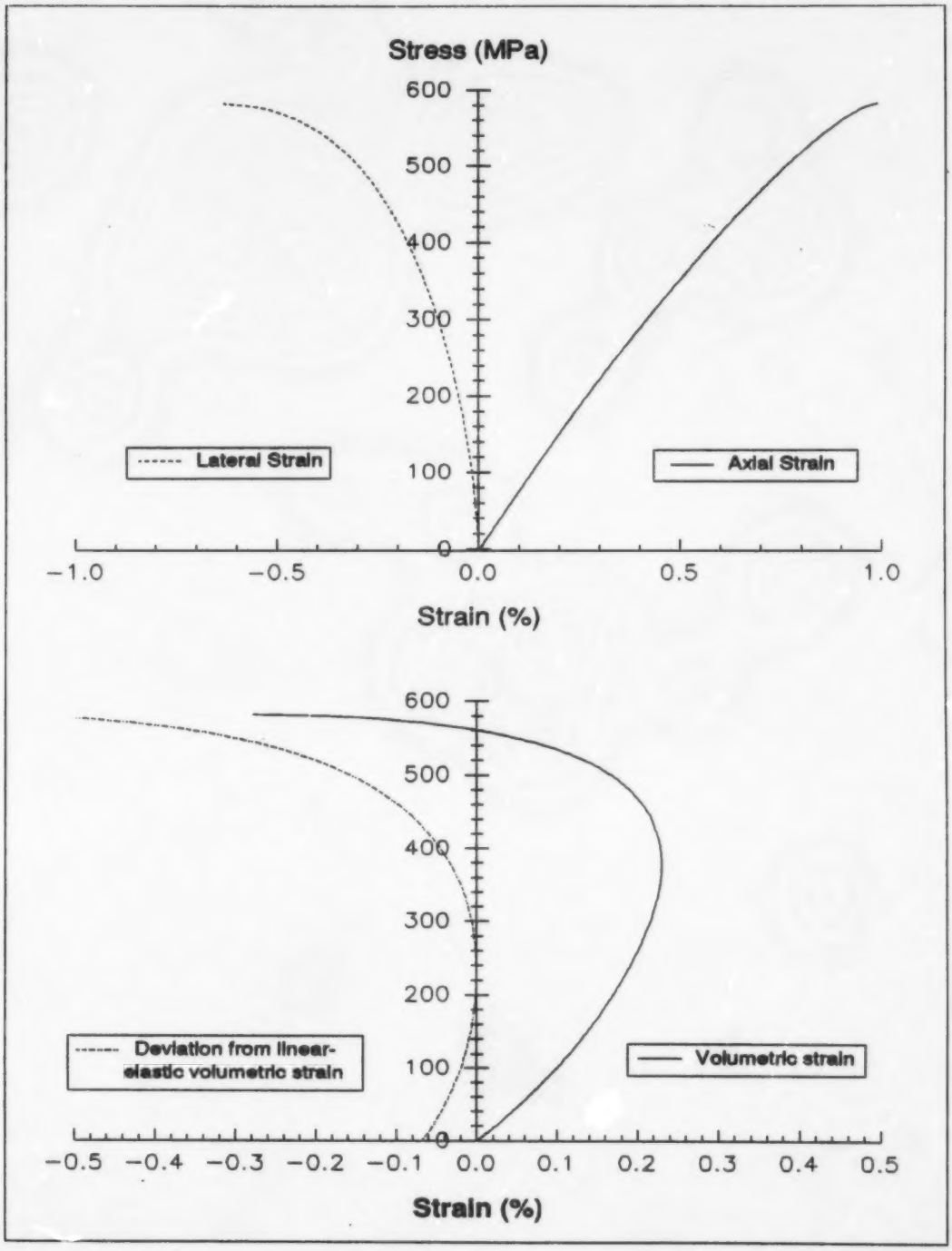

Figure A19 - Stress/strain curves for sample no. 11.367

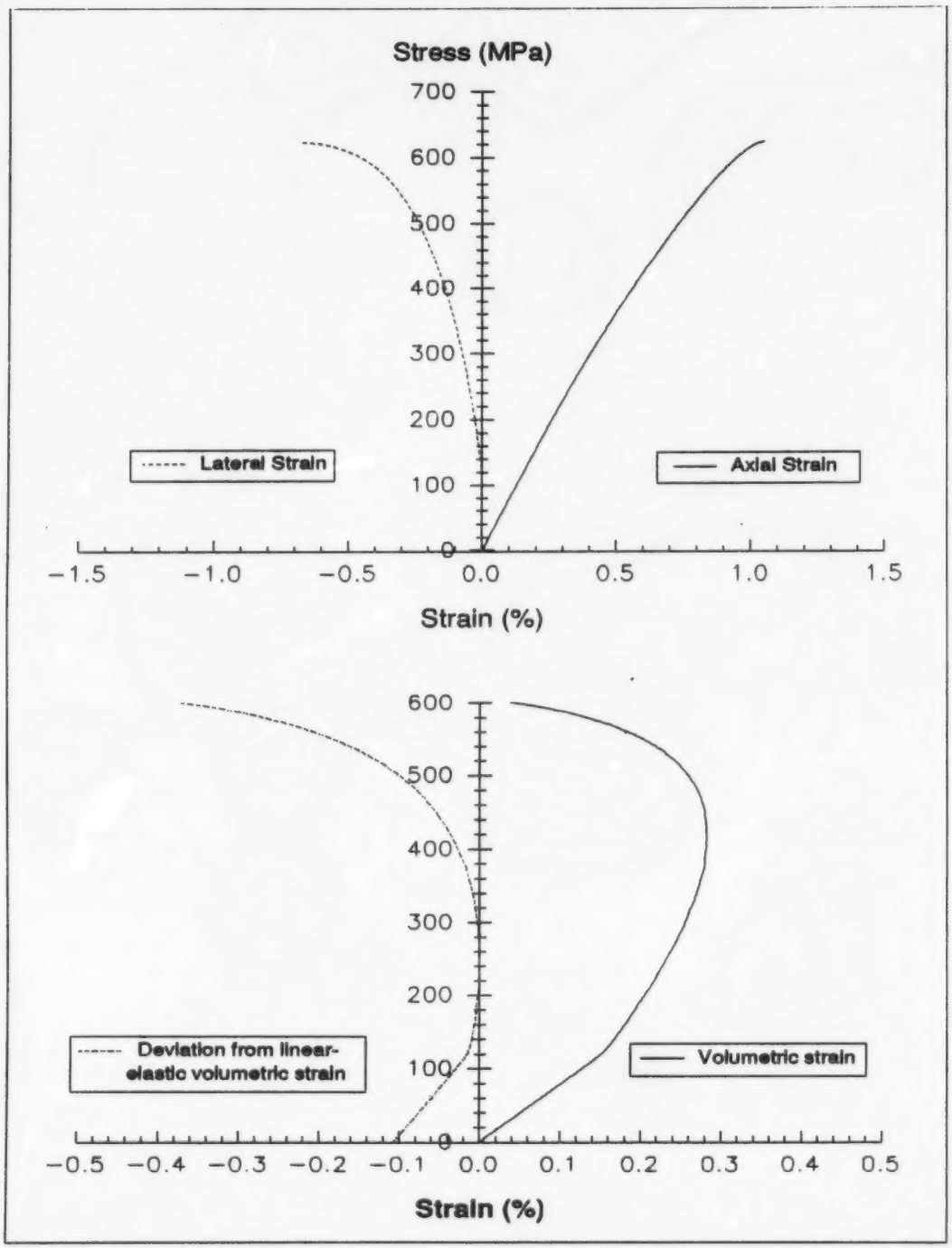

Figure A20 - Stress/strain curves for sample no. 11.475

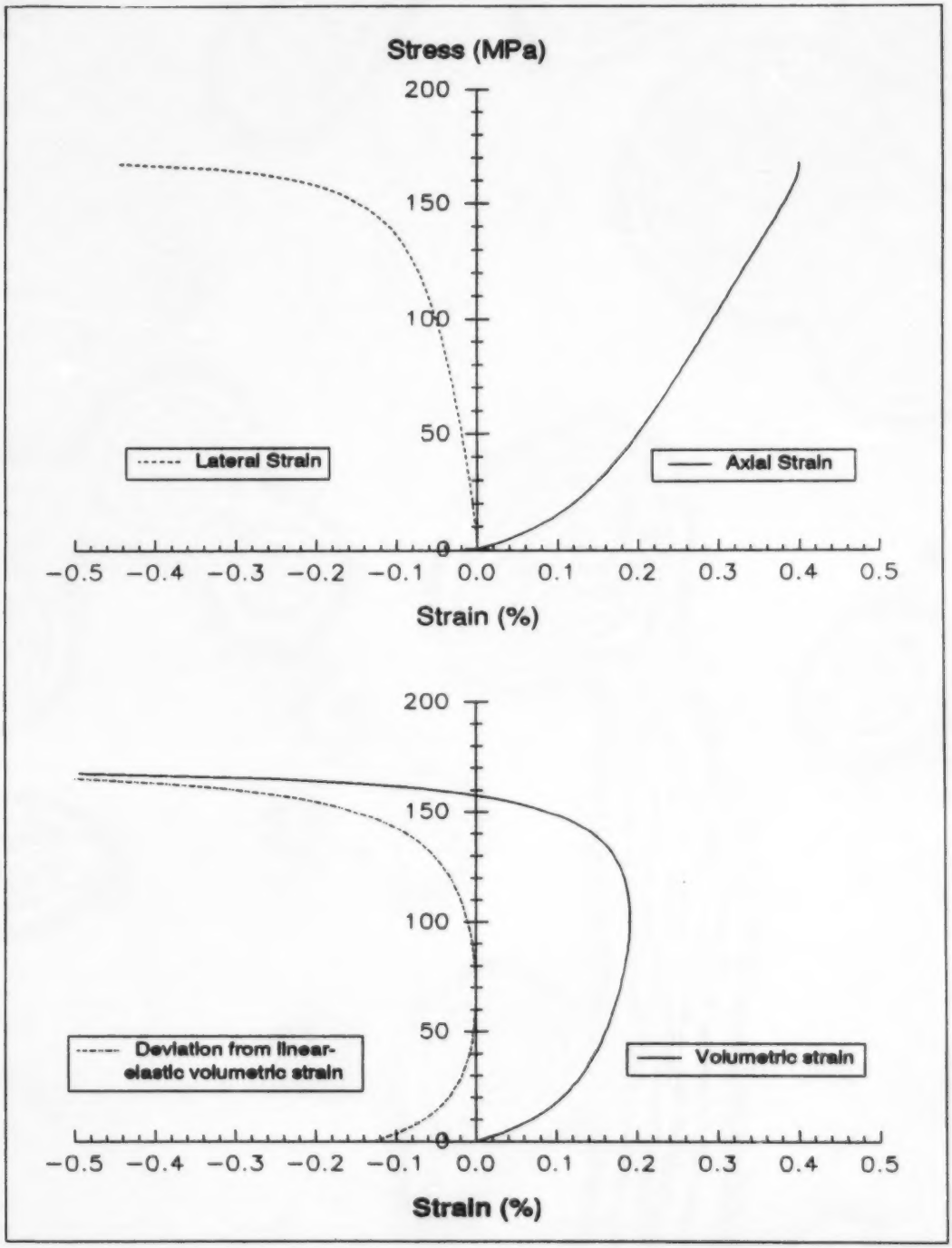

Figure A21 - Stress/strain curves for sample no. 11.650

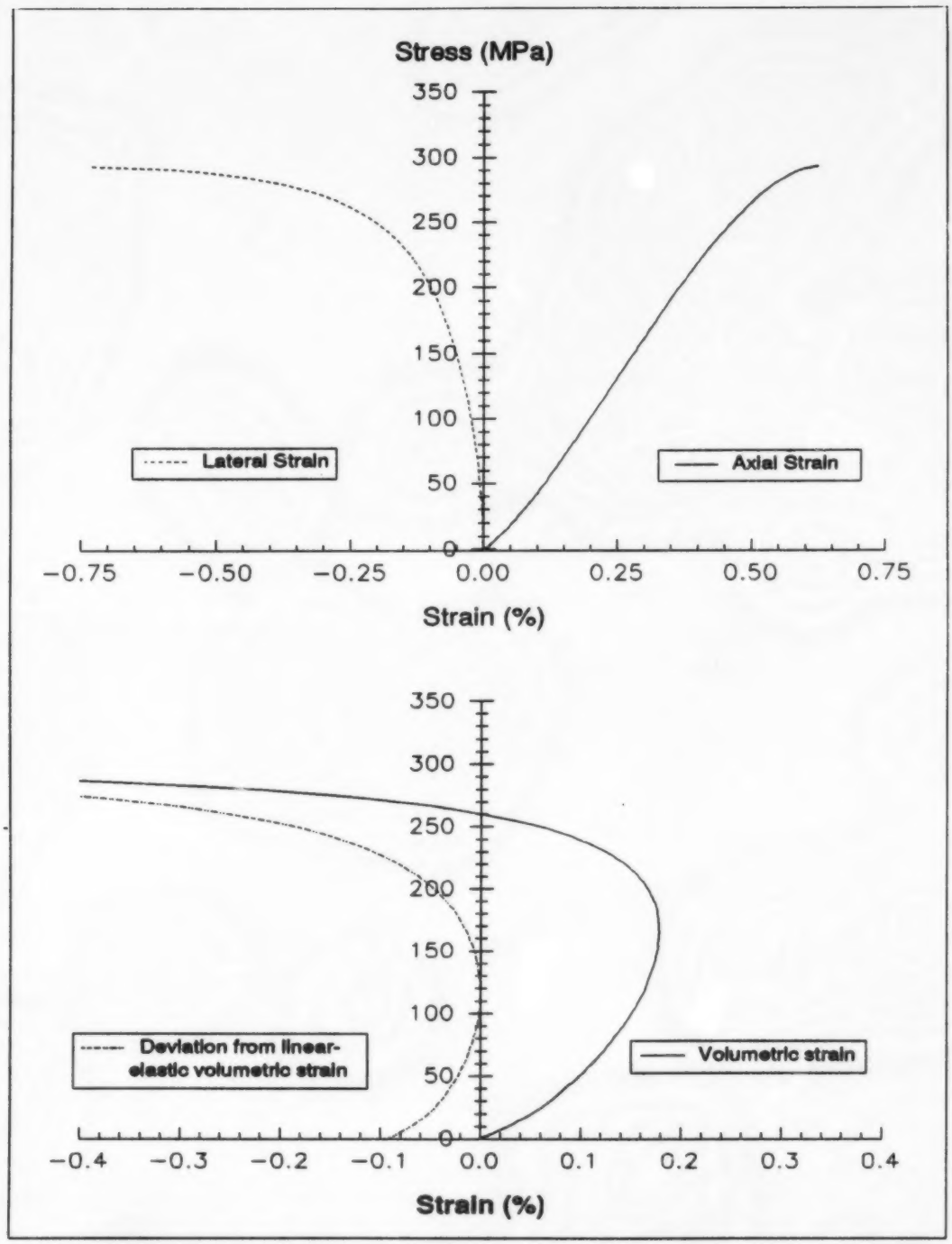

Figure A22 - Stress/strain curves for sample no. 11.759

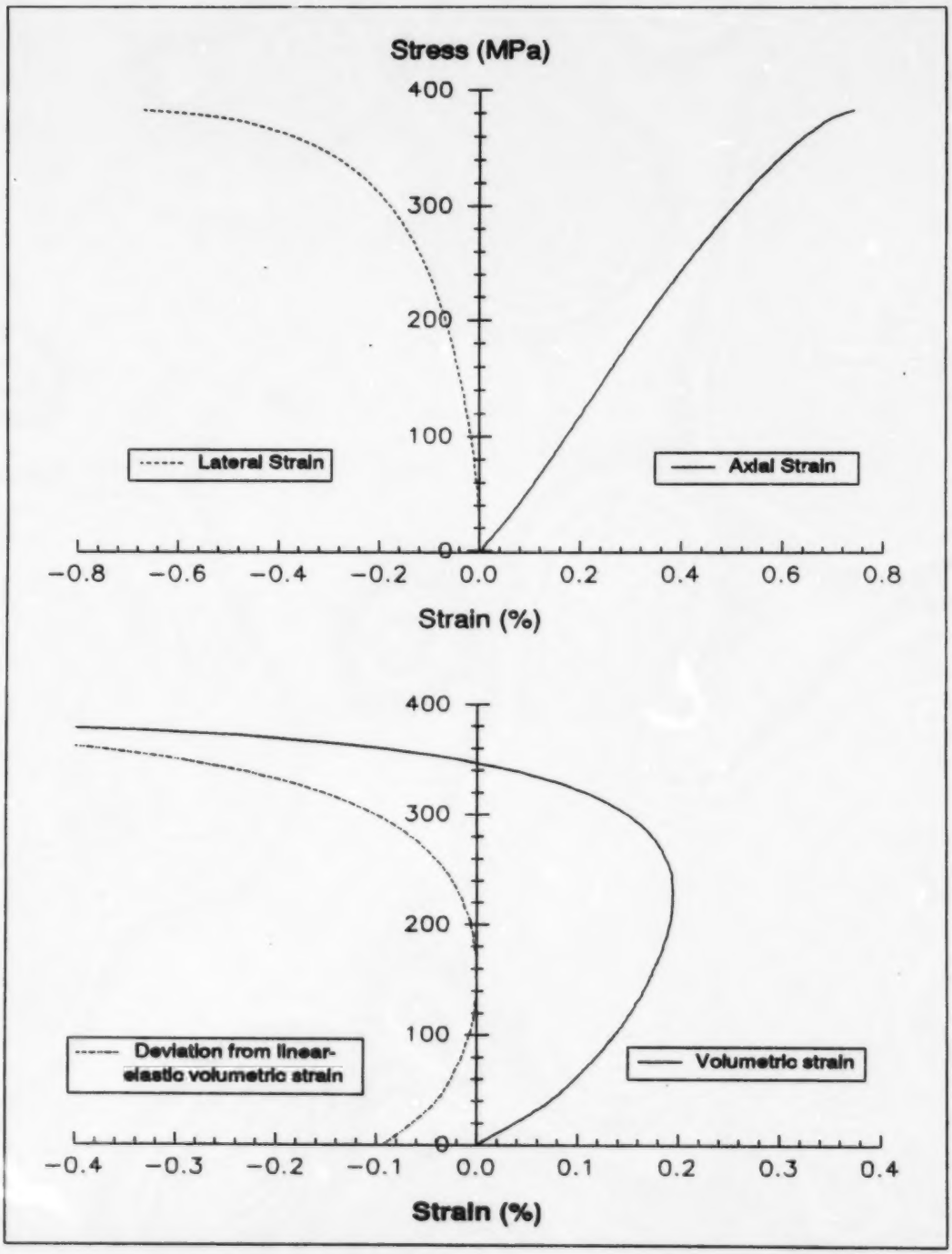

Figure A23 - Stress/strain curves for sample no. 11.865

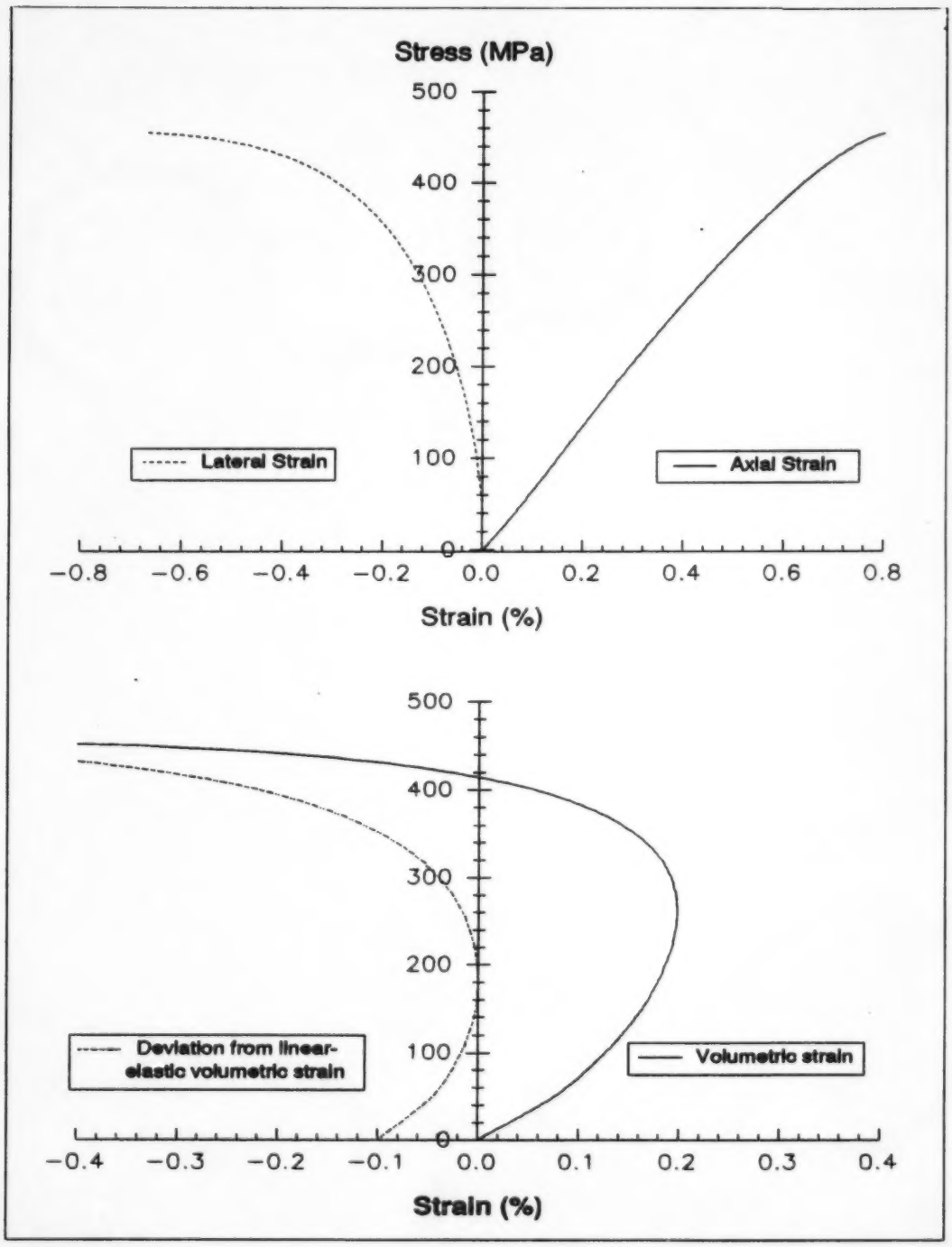

Figure A24 - Stress/strain curves for sample no. 12.421

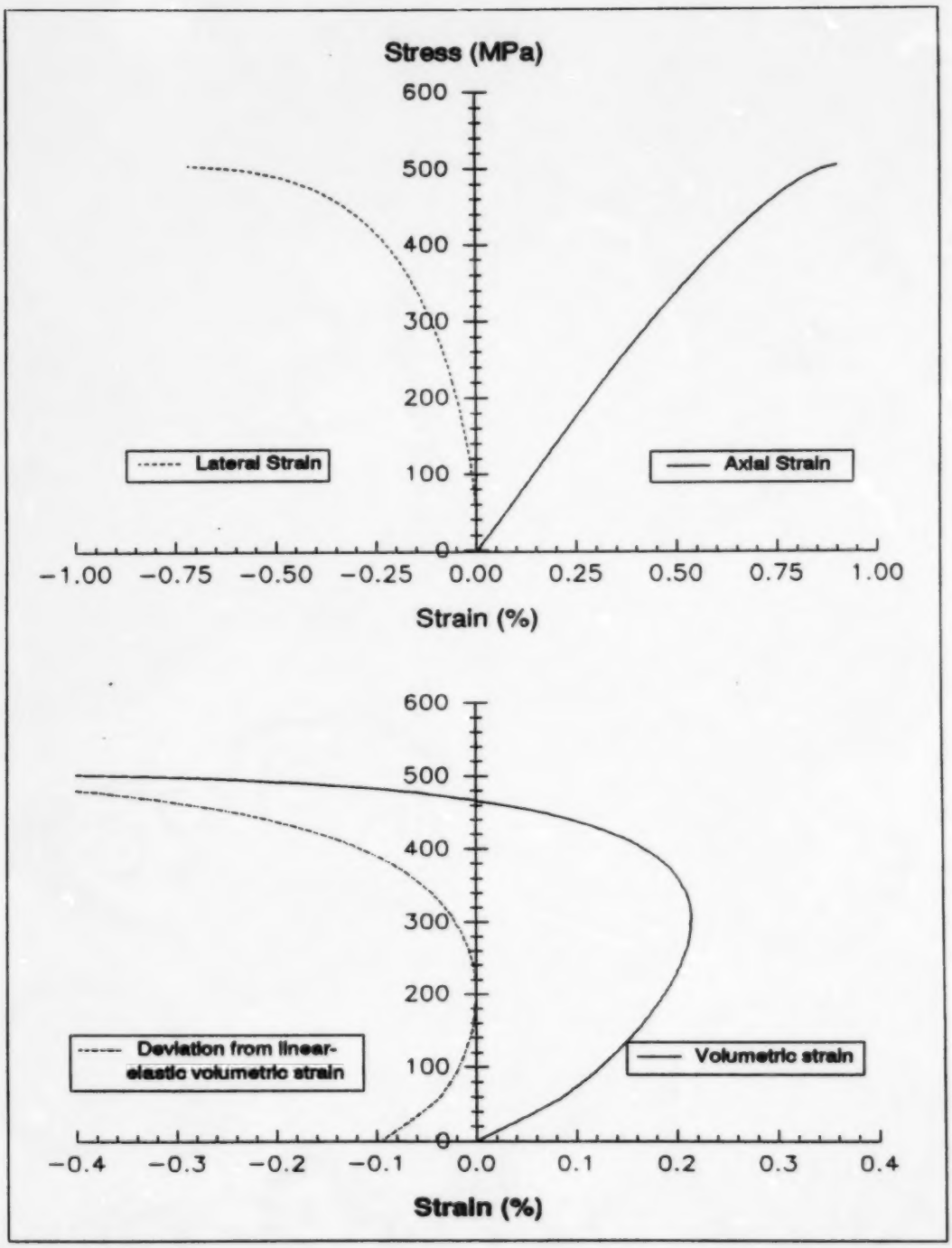

Figure A25 - Stress/strain curves for sample no. 12.532

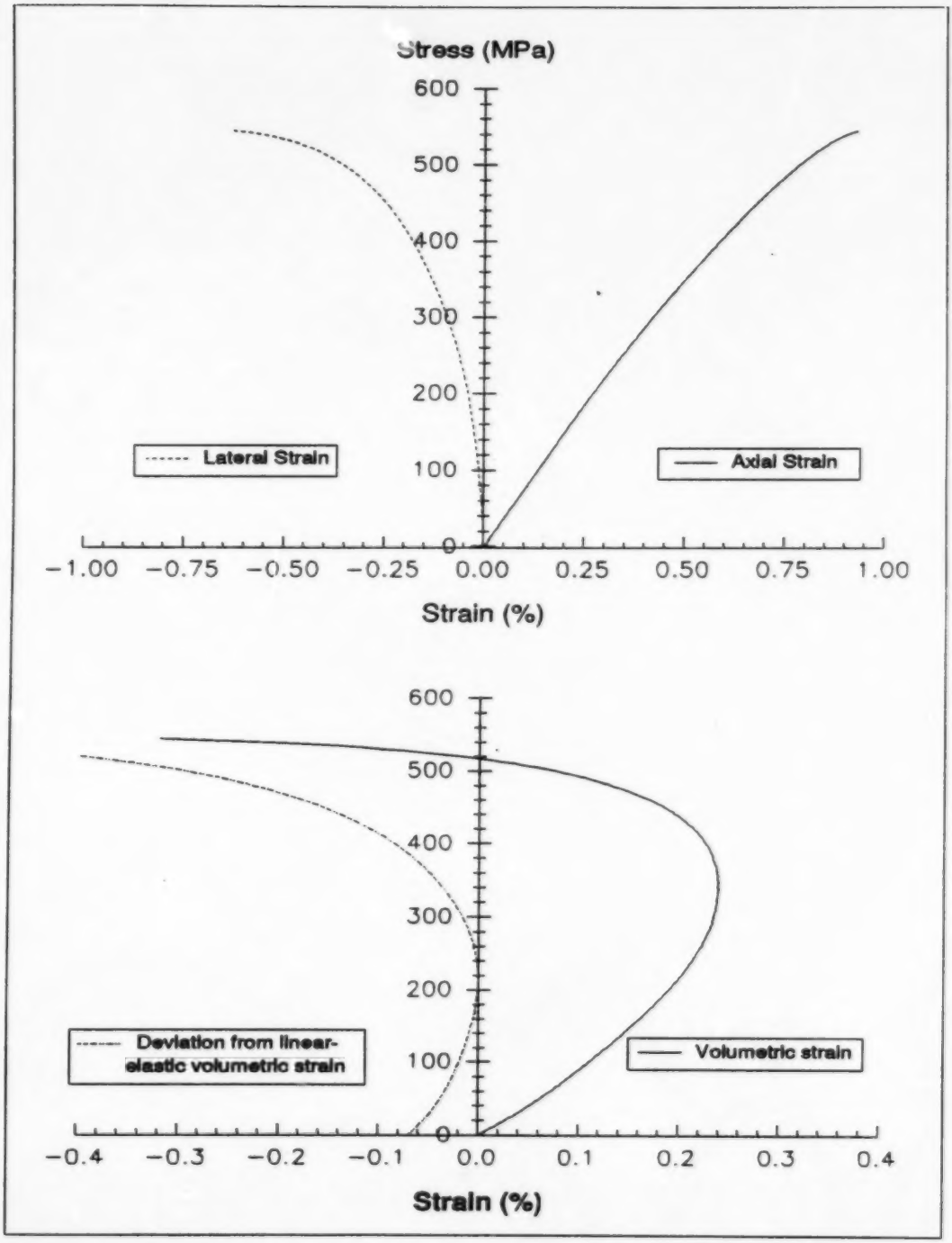

Figure A26 - Stress/strain curves for sample no. 12.635

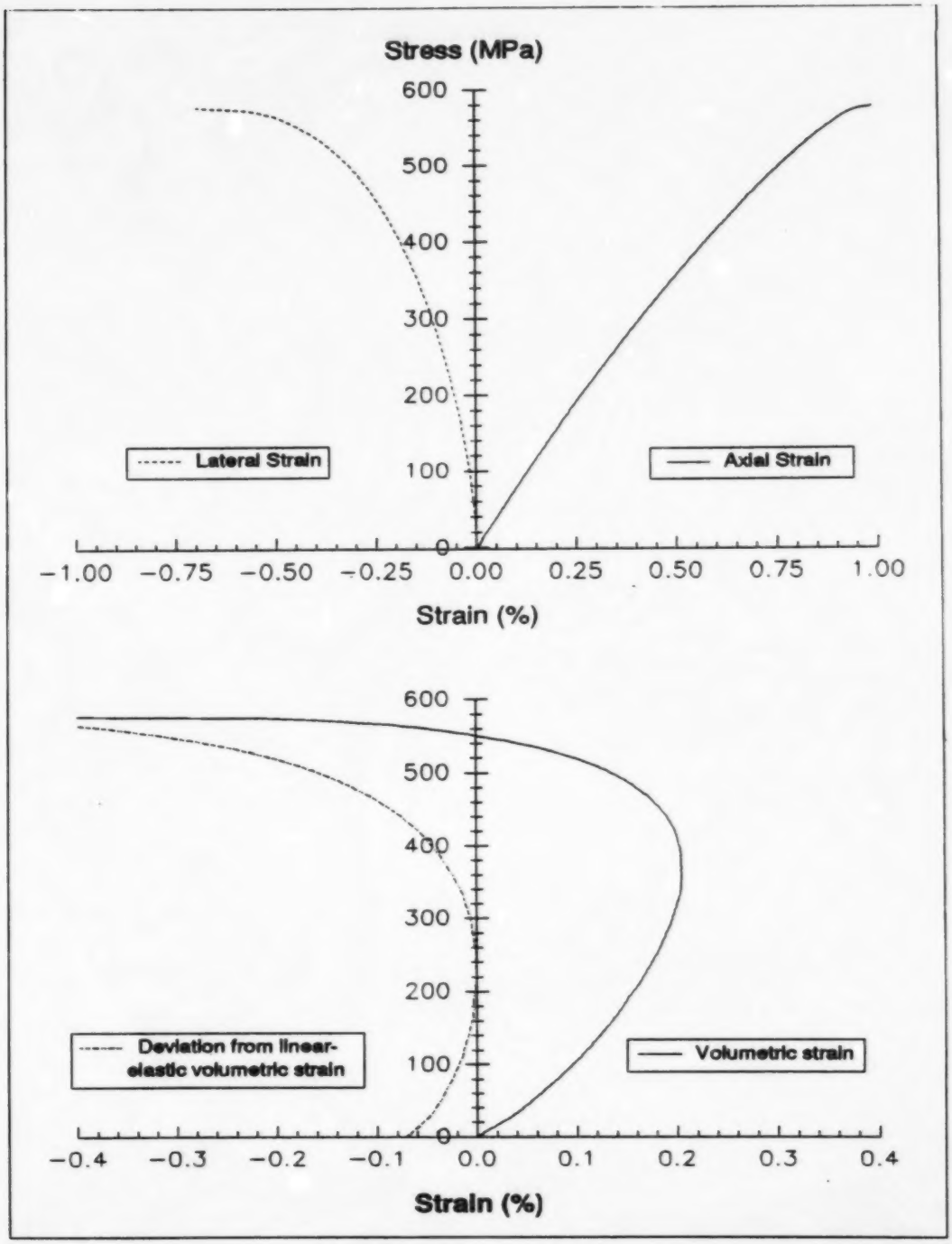

Figure A27 - Stress/strain curves for sample no. 12.744

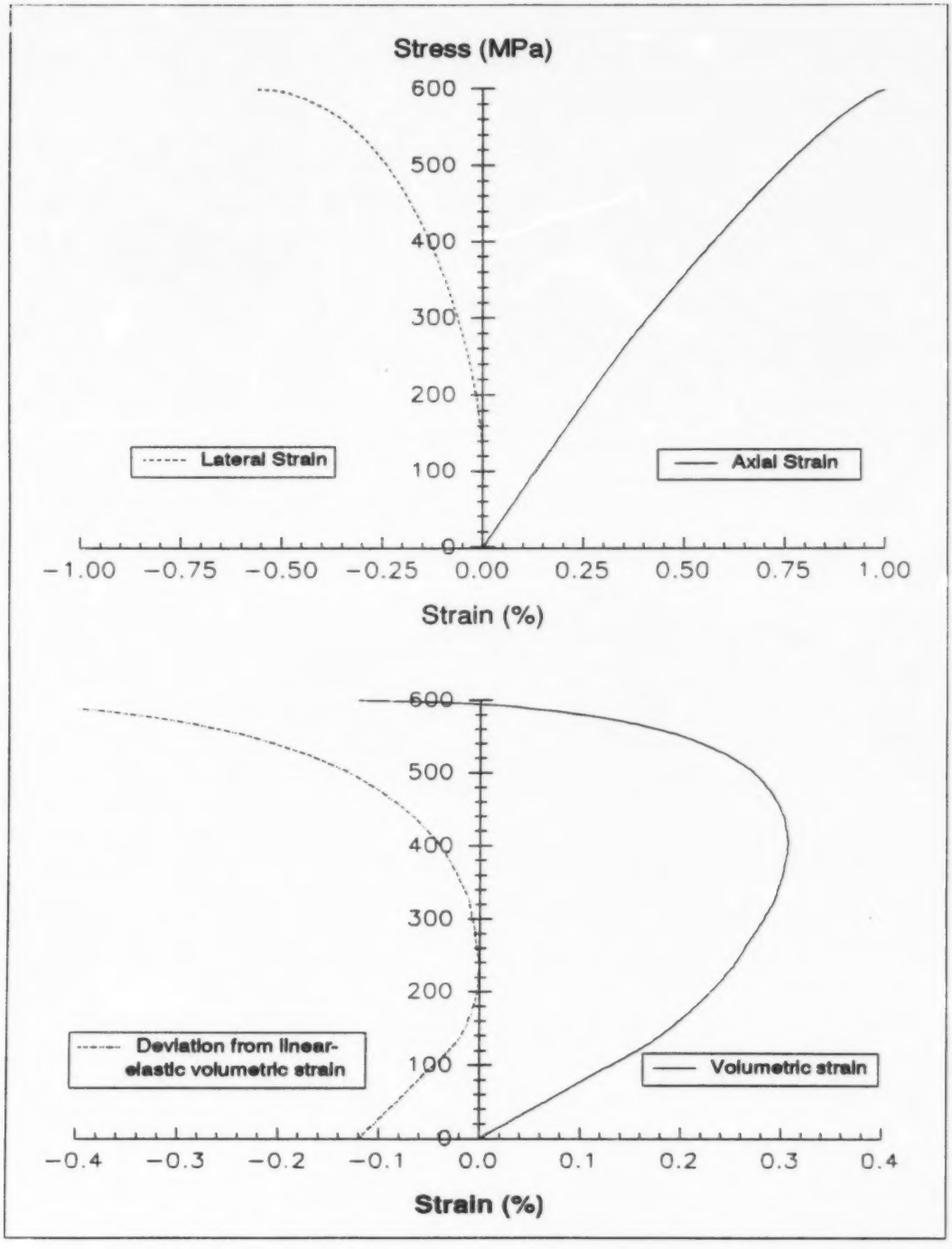

Figure A28 - Stress/strain curves for sample no. 12.849